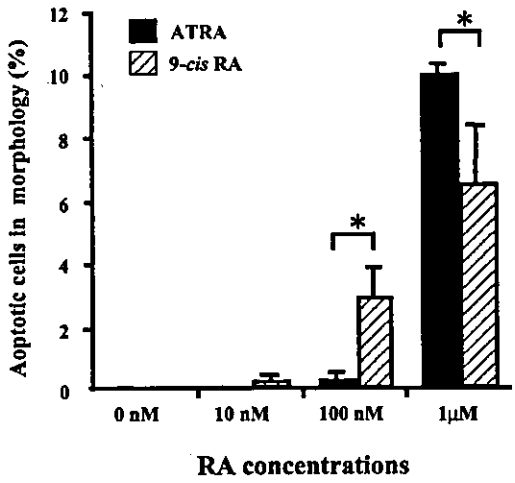

Fig. 3. Apoptotic morphology of UF-1 cells treated with ATRA or 9CRA. After 8 days of culture in the absence or presence of different concentrations of ATRA or 9CRA, UF-1 cells were examined for morphological features of apoptosis. Bars are mean ± S.D. of three experiments (* $P < 0.05$).

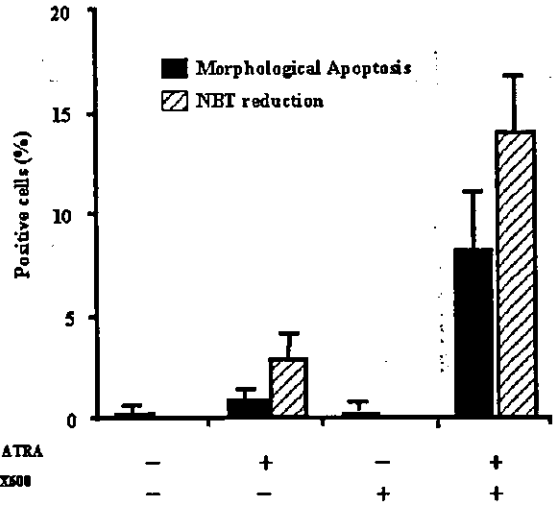

Fig. 5. Apoptosis of and NBT reduction by UF-1 cultured for 7 days in the absence or presence of 100 nM ATRA or 1 μM HX600, or both. Bars indicate mean ± S.D. of three experiments.

PML-RARα chimeric gene (data not shown). To assess ligand-dependent transcriptional activity of the mutant protein in comparison with that of the wild-type, we performed transient transfection experiments. Increased transcription of the reporter constructs was observed when cells expressing wild-type PML-RARα were treated with various concentrations of ATRA or 9CRA alone. Although cells expressing mutant PML-RARα showed increased transcription in response only to 1 μM ATRA, the level reached only that of the wild-type PML-RARα stimulated by 10 nM ATRA (Fig. 6). There was no significant difference between ATRA and 9CRA for RA-dependent transcriptional activity of the mutant protein, and the combination of HX600 and ATRA had no effect on the response of mutant PML-RARα to RA (Fig. 6A–C). Furthermore, when cells were co-transfected with vectors expressing normal RARα and PML-RARα, the mutant protein showed significantly higher dominant-negative inhibition of RARα in comparison with that of wild-type PML-RARα (Fig. 6D).

3.6. Three-color FACS analysis of early apoptotic cells

To detect cells in early apoptosis, the percentages of dead cells or viable, mature cells were analyzed during ATRA-induced differentiation and apoptosis (Fig. 7). In the presence of 1 μM ATRA, the percentage of CD11b (+), PI (−) viable, mature cells gradually increased over a period of 6 days, and then the number of PI (+) dead cells increased gradually (Fig. 8A). A small fraction (5.0 ± 0.4%) of early apoptotic cells with annexin V (+), PI (−) phenotypes were

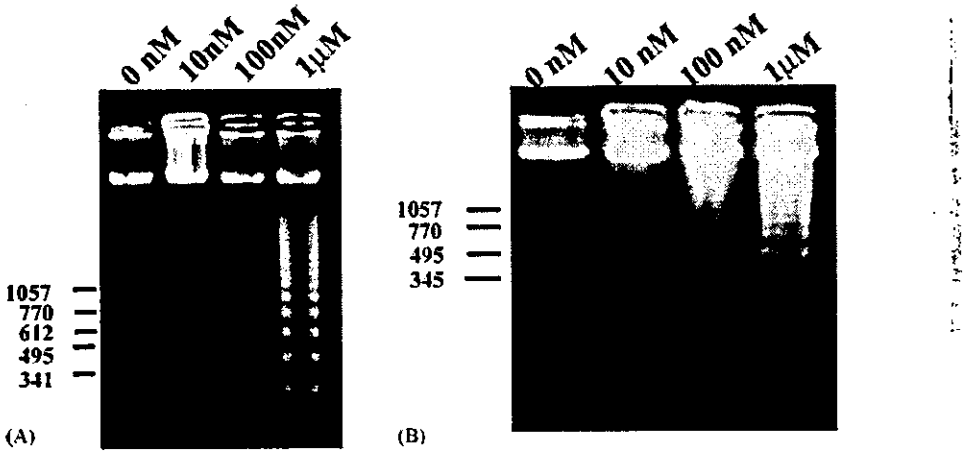

Fig. 4. DNA fragmentation in UF-1 cells treated with ATRA (A) or 9CRA (B). Total DNA was extracted from UF-1 cells cultured for 7 days in the absence or presence of various concentrations of ATRA or 9CRA and then separated by electrophoresis in 2% agarose gels. Markers are shown in bp in size.

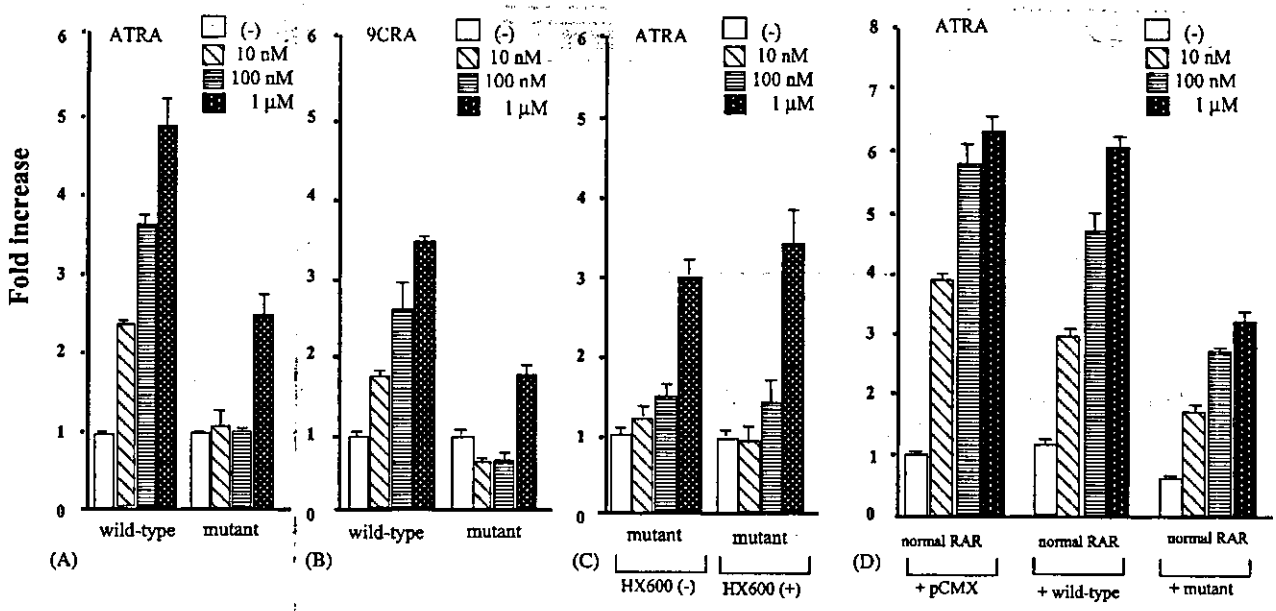

Fig. 6. Ligand-dependent transcriptional activities of wild-type or mutant PML-RARα proteins. Luciferase and β-gal reporter constructs were co-transfected with expression vector encoding wild-type or mutant PML-RARα into COS-1 cells, and the cells were cultured in the absence or presence of various concentrations of ATRA (A) or 9CRA (B) or the combination of 100 nM ATRA with 1 μM HX600 (C). To evaluate the dominant-negative effect of PML-RARα on normal RARα activity, vector expressing normal RARα was co-transfected with vector expressing wild-type or mutant PML-RARα (D). Luciferase activity was normalized to β-gal activity and expressed as fold-increase of activities in the absence of retinoids.

detected after 6 days when the cells started to show morphologic features consistent with apoptosis. Interestingly, approximately 50% of the annexin V (+), PI (−) cells did not express CD11b (Fig. 8B). Furthermore, annexin V (+), PI (−), CD11b (−) UF-1 cells sorted after 8 days culture in the presence of 1 μM ATRA showed immature morphology (Fig. 8C).

4. Discussion

In the present study, we showed that UF-1 cells had a unique response to RA at the cellular level. RA sensitivity was markedly altered in connection with the dose and time of RA treatment. UF-1 cells were unresponsive to ATRA at doses ≤100 nM, but showed growth inhibition, differentiation and apoptosis in response to 1 μM ATRA. UF-1 cells showed a similar but more sensitive response to 9CRA. Interestingly, the reduced sensitivity of UF-1 cells to RA was obvious within 4 days of ATRA treatment, but we found that culture with 1 μM ATRA for longer periods induced UF-1 cells to undergo growth inhibition, differentiation and apoptosis.

It is likely that the impaired cellular response to ≤100 nM ATRA is due to the mutant PML-RARα, because the UF-1 cell line was established from an ATRA-resistant APL patient with the mutation at relapse. Furthermore, the mutant PML-RARα protein showed no transcriptional activity in response to ≤100 nM ATRA and lacked ATRA binding [25,30]. However, it is not clear how APL cells with the mutant PML-RARα can respond to 1 μM ATRA when exposed for longer times. To assess this question, we compared RA responses of UF-1 cells with those of the mutant PML-RARα as assessed by RA-dependent transcriptional activity in vitro.

In response to 1 μM ATRA, ≥100 nM 9CRA, or 1 μM HX600 in combination with ATRA, UF-1 cells showed morphological and functional maturation. By contrast, the extents of in vitro transcriptional activity of mutant PML-RARα in response to the same conditions were as low as that of wild-type PML-RARα in response to 10 nM RA and had no influence by HX600. Therefore, it is suggested that there are differences between the cellular response of UF-1 to RA and the molecular response of mutant PML-RARα. Furthermore, mutant PML-RARα had an increase in dominant-negative effect on the RA-dependent transcriptional activity of normal RARα as compared with that by wild-type PML-RARα. Therefore, the response of UF-1 cells can not be due to the response of the mutant PML-RARα, suggesting that signaling pathways other than that of the mutant protein may alter the UF-1 response to 1 μM ATRA.

Although the mechanism that underlies APL cell maturation remains unclear, it is thought that PML-RARα causes a differentiation block that can be released by RARα agonist [31]. In this context, the response of APL cells expressing mutant PML-RARα may be determined primarily by the altered response of mutant PML-RARα to RA. An in vitro transfection study revealed that patient-derived PML-RARα carrying distinct mutations have diverse effect

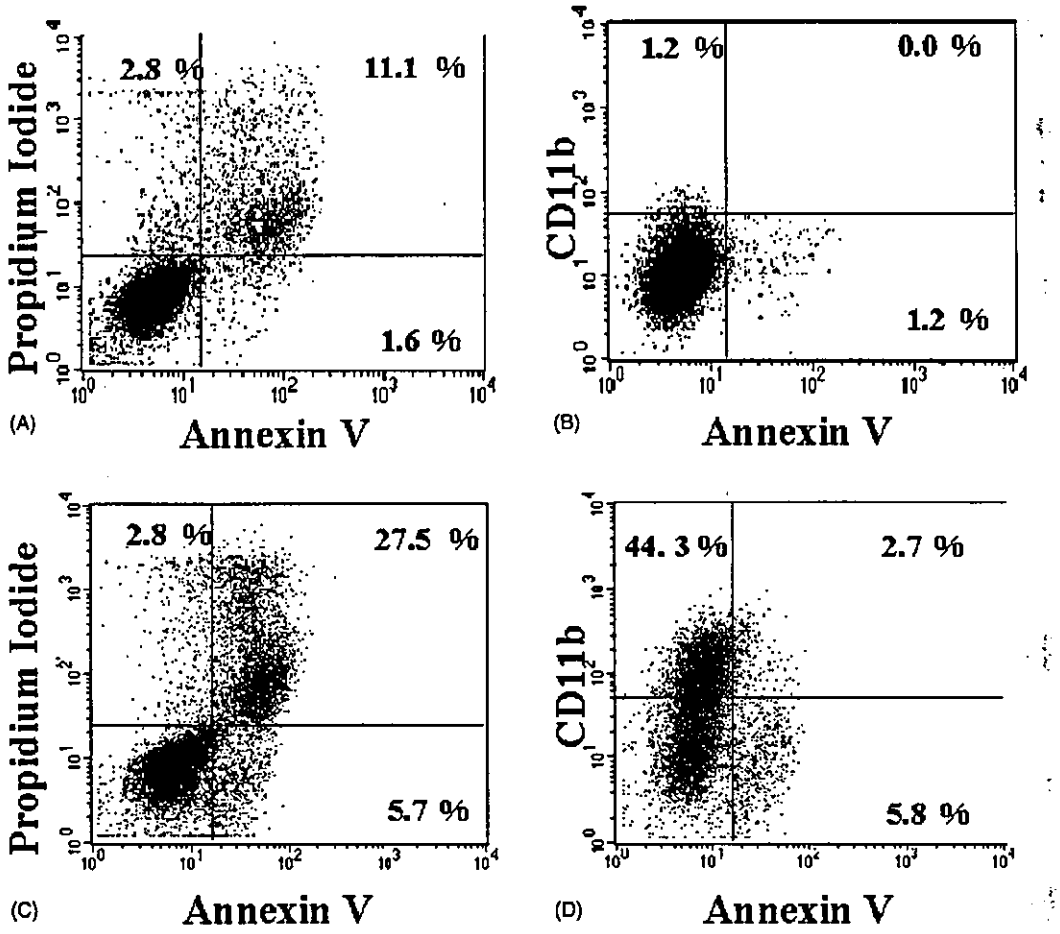

Fig. 7. Flow cytometric detection of undifferentiated early-apoptotic cells. UF-1 cells were cultured for 6 days in the absence (A, B) or presence (C, D) of 1 μM ATRA and then stained with PI, annexin V, and anti-CD11b antibody. The proportion of early-apoptotic cells with the annexin V (+), PI (−) phenotype were analyzed among the whole cell population (A, C). After gating PI (−) viable cells, undifferentiated early-apoptotic cells with the annexin V (+), CD11b (−) phenotype were analyzed in the gated populations (B, D).

on RA-dependent transcriptional regulation [15]. It was reported that the Arg611Trp mutant PML-RARα does neither release the co-repressor SMRT nor recruit co-activator ACTR even when stimulated with ≥1 μM ATRA, whereas the mutant PML-RARα retained the ability to interact with DRIP, a ligand-dependent transcription activators of vitamin D_3 receptor, with RA sensitivity similar to that of wild-type PML-RARα [16,32].

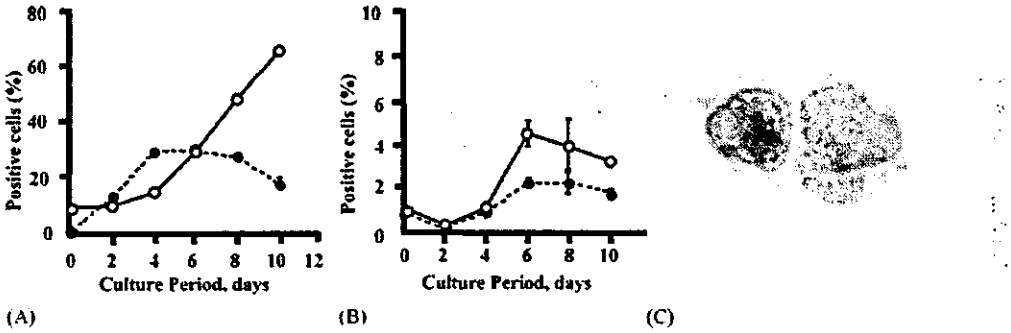

Fig. 8. Three-color cytometric analysis of UF-1 cells stained for annexin V, CD11b, and PI. (A) Chronological changes in proportion of PI (+) dead cells (○) or viable CD11b (+), PI (−) differentiating cells (●). Results are mean ± S.D. of three expreiments. (B) Among the gated PI (−) viable cells, chromological changes in proportion of annexin V (+) early-apoptosic cells (○) or undifferentiated annexin V (+), CD11b (−) early-apoptotic cells (●) were evaluated. Results are mean ± S.D. of three expreiments. (C) Morphology of annexin V (+), CD11b (−) UF-1 cells stained with Wright-Giemsa (1000× magnification).

There have been two reports of the cellular response of primary cultures of APL cells with distinct mutations in PML-RARα [14,17]. Such APL cells may be categorized into two groups: (1) APL cells with moderately decreased responses to 1 μM ATRA by day 4 and partially reduced ATRA binding and (2) cells with little response to 1 μM ATRA by day 4 and almost complete loss of ATRA binding. Although UF-1 cells seem to belong to the latter category, it needs further investigation to know whether patient-derived APL cells with features of the latter category would have an altered RA response similar to that of UF-1.

It should be noted that UF-1 cells gradually underwent maturation with subsequent apoptosis after 4 days of treatment with 1 μM ATRA. However, it is not known how UF-1 cells would respond to ATRA if UF-1 cells have had wild-type PML-RARα protein instead of the mutant. This time course of RA response of UF-1 cells is relatively slow if compared with that of HL-60 or NB4 cells, which show a maximal response by day 4 [33,34], suggesting that RA signaling other than that through PML-RARα may underlay the delayed response of UF-1 to 1 μM ATRA. Recently, it was shown that RARβ is upregulated in response to RA stimulation and is involved in RA-induced apoptosis of tumor cells [35]. Thus, activation of RARβ may play a role in the delayed RA response of UF-1, although further analyses are needed.

The response of APL to RA may be regulated by signals other than PML-RARα. Fanelli et al. [36] showed that the sensitivity of APL cells to RA is altered by the proteosome pathway through constitutive degradation of PML-RARα protein. Moreover, Benoit et al. [37] reported the existence of an RARα-independent RXR signaling pathways, in which a combination of RXR agonists and protein kinase A stimulators induce differentiation of ATRA-sensitive and ATRA-resistant NB4 cells without degradation of PML-RARα protein or reconstitution of PML nuclear bodies. Alternatively, post-transcriptional modification through covalent binding of RA to cellular proteins, a process called "retinoylation", may be involved in the RA response of UF-1 cells [38]. Further studies are needed.

ATRA at pharmacological doses can restore RA signaling in APL cells by releasing the dominant-negative effect of PML-RARα, leading to maturation and subsequent death of cells via apoptosis. However, hematological findings in patients who had undergone ATRA therapy suggested that APL cells can be induced to undergo apoptosis as a consequence of maturation, and independent of differentiation [23]. Interestingly, in the presence of 1 μM ATRA, we detected a small fraction of viable UF-1 cells that were annexin V-positive, CD11b-negative, and morphologically immature, indicating that a portion of the ATRA-treated APL was in the early stage of apoptosis. UF-1 cells may be predisposed to undergo apoptosis independent of differentiation as observed in response to stimuli involving the STAT signal pathway [39] or prior to terminal differentiation in response to arsenic trioxide [8]. This separation of apoptosis from differentiation in RA-treated APL suggest that there may be a cellular imbalance in the restored functions of proteins such as normal RARα and PML restored by ATRA [20,40].

In conclusion, the UF-1 cell line, which was established from a patient with ATRA resistance, may be of great value for investigating the relation between the cellular and molecular responses to ATRA of APL with mutant PML-RARα chimeric gene. Moreover, this cell line may be useful for elucidating the mechanism(s) by which APL cells are induced into apoptosis independent of differentiation.

Acknowledgements

This study was supported by grants from the Ministry of Education, Science and Culture, and the Ministry of Health and Public Welfare, Japan. We thank Dr. T.R. Breitman for helpful advice.

References

[1] Perez A, Kastner P, Sethi S, Lutz Y, Reibel C, Chambon P. PMLRAR homodimers: distinct DNA binding properties and heteromeric interactions with RXR. EMBO J 1993;12:3171–82.
[2] Grignani F, De Matteis S, Nervi C, Tomassoni L, Gelmetti V, Cioce M, et al. Fusion proteins of the retinoic acid receptor-α recruit histone deacetylase in promyelocytic leukaemia. Nature 1998;391:815–8.
[3] Chen ZX, Xue YQ, Zhang R, Tao RF, Xia XM, Li C, et al. A clinical and experimental study on all-*trans* retinoic acid-treated acute promyelocytic leukemia patients. Blood 1991;78:1413–9.
[4] Warrell RPJ, Frankel SR, Miller WHJ, Scheinberg DA, Itri LM, Hittelman WN. Differentiation therapy of acute promyelocytic leukemia with tretinoin (all-*trans*-retinoic acid). N Engl J Med 1991; 324:1385–93.
[5] Cornic M, Chomienne C. Induction of retinoid resistance by all-*trans* retinoic acid in acute promyelocytic leukemia after remission. Leuk Lymphoma 1995;18:249–57.
[6] Degos L, Dombret H, Chomienne C, Daniel MT, Miclea JM, Chastang C, et al. All-*trans*-retinoic acid as a differentiating agent in the treatment of acute promyelocytic leukemia. Blood 1995;85:2643–53.
[7] Shen ZX, Chen GQ, Ni JH, Li XS, Xiong SM, Qiu QY, et al. Use of arsenic trioxide (As_2O_3) in the treatment of acute promyelocytic leukemia (APL): II. Clinical efficacy and pharmacokinetics in relapsed patients. Blood 1997;89:3354–60.
[8] Soignet SL, Maslak P, Wang ZG, Jhanwar S, Calleja E, Dardashti LJ. Complete remission after treatment of acute promyelocytic leukemia with arsenic trioxide. N Engl J Med 1998;339:1341–8.
[9] Delva L, Cornic M, Balitrand N, Guidez F, Miclea JM, Delmer A, et al. Resistance to all-*trans* retinoic acid (ATRA) therapy in relapsing acute promyelocytic leukemia: study of in vitro ATRA sensitivity and cellular retinoic acid binding protein levels in leukemic cells. Blood 1993;82:2175–81.
[10] Kizaki M, Ueno H, Yamazoe Y, Shimada M, Takayama N, Muto A, et al. Mechanisms of retinoid resistance in leukemic cells: possible role of cytochrome P450 and *P*-glycoprotein. Blood 1996;87:725–33.
[11] Kizaki M, Ueno H, Matsushita H, Takayama N, Muto A, Awaya N, et al. Retinoid resistance in leukemic cells. Leuk Lymphoma 1997;25:427–34.
[12] Shao W, Benedetti L, Lamph WW, Nervi C, Miller WHJ. A retinoid-resistant acute promyelocytic leukemia subclone expresses a dominant negative PML-RARα mutation. Blood 1997;89:4282–9.

[13] Imaizumi M, Suzuki H, Yoshinari M, Sato A, Saito T, Sugawara A, et al. Mutations in the E-domain of RAR portion of the PML/RAR chimeric gene may confer clinical resistance to all-*trans* retinoic acid in acute promyelocytic leukemia. Blood 1998;92:374–82.
[14] Ding W, Li YP, Nobile LM, Grills G, Carrera I, Paietta E, et al. Leukemic cellular retinoic acid resistance and missense mutations in the PML-RARα fusion gene after relapse of acute promyelocytic leukemia from treatment with all-*trans* retinoic acid and intensive chemotherapy. Blood 1998;92:1172–83.
[15] Cote S, Zhou D, Bianchini A, Nervi C, Gallagher RE, Miller Jr WH. Altered ligand binding and transcriptional regulation by mutations in the PML/RARα ligand-binding domain arising in retinoic acid-resistant patients with acute promyelocytic leukemia. Blood 2000;96:3200–8.
[16] Cote S, Rosenauer A, Bianchini A, Seiter K, Vandewiele J, Nervi C, et al. Response to histone deacetylase inhibition of novel PML/RARα mutants detected in retinoic acid-resistant APL cells. Blood 2002;100:2586–96.
[17] Zhou DC, Kim SH, Ding W, Schultz C, Warrell Jr RP, Gallagher RE. Frequent mutations in the ligand-binding domain of PML-RARα after multiple relapses of acute promyelocytic leukemia: analysis for functional relationship to response to all-*trans* retinoic acid and histone deacetylase inhibitors in vitro and in vivo. Blood 2002;99:1356–63.
[18] Robertson KA, Emami B, Collins SJ. Retinoic acid-resistant HL-60R cells harbor a point mutation in the retinoic acid receptor ligand-binding domain that confers dominant negative activity. Blood 1992;80:1885–9.
[19] Li YP, Said F, Gallagher RE. Retinoic acid-resistant HL-60 cells exclusively contain mutant retinoic acid receptor-alpha. Blood 1994;83:3298–302.
[20] Duprez E, Benoit G, Flexor M, Lillehaug JR, Lanotte M. A mutated PML/RARA found in the retinoid maturation resistant NB4 subclone, NB4-R2, blocks RARA and wild-type PML/RARA transcriptional activities. Leukemia 2000;14:255–61.
[21] Vyas RC, Frankel SR, Agbor P, Miller WHJ, Warrell RPJ, Hittelman WN. Probing the pathobiology of response to all-*trans* retinoic acid in acute promyelocytic leukemia: premature chromosome condensation/fluorescence in situ hybridization analysis. Blood 1996;87:218–26.
[22] Savill J, Fadok V, Henson P, Haslett C. Phagocyte recognition of cells undergoing apoptosis. Immunol Today 1993;14:131–6.
[23] Sato A, Imaizumi M, Saito T, Yoshinari M, Suzuki H, Hayashi Y, et al. Detection of apoptosis in acute promyelocytic leukemia cells in vivo during differentiation-induction with all-*trans* retinoic acid in combination with chemotherapy. Leuk Res 1999;23:827–32.
[24] Kizaki M, Matsushita H, Takayama N, Muto A, Ueno H, Awaya N, et al. Establishment and characterization of a novel acute promyelocytic leukemia cell line (UF-1) with retinoic acid-resistant features. Blood 1996;88:1824–33.
[25] Takayama N, Kizaki M, Hida T, Kinjo K, Ikeda Y. Novel mutation in the PML/RARα chimeric gene exhibits dramatically decreased ligand-binding activity and confers acquired resistance to retinoic acid in acute promyelocytic leukemia. Exp Hematol 2001;29:864–72.
[26] Umemiya H, Kagechika H, Fukasawa H, Kawachi E, Ebisawa M, Hashimoto Y, et al. Action mechanism of retinoid-synergistic dibenzodiazepines. Biochem Biophys Res Commun 1997;233:121–5.
[27] Imaizumi M, Sato A, Koizumi Y, Inoue S, Suzuki H, Suwabe N, et al. Potentiated maturation with a high proliferating activity of acute promyelocytic leukemia induced in vitro by granulocyte or granulocyte/macrophage colony-stimulating factors in combination with all-*trans* retinoic acid. Leukemia 1994;8:1301–8.
[28] Vermes I, Haanen C, Steffens Nakken H, Reutelingsperger CP. A novel assay for apoptosis. Flow cytometric detection of phosphatidylserine expression on early apoptotic cells using fluorescein labelled Annexin V. J Immunol Methods 1995;184:39–51.
[29] Tominaga T, Kure S, Yoshimoto T. DNA fragmentation in focal cortical freeze injury of rats. Neurosci Lett 1992;139:265–8.
[30] Marasca R, Zucchini P, Galimberti S, Leonardi G, Vaccari P, Donelli A, et al. Missense mutations in the PML/RARα ligand binding domain in ATRA-resistant As(2)O(3) sensitive relapsed acute promyelocytic leukemia. Haematologica 1999;84:963–8.
[31] Slack JL, Gallagher RE. The molecular biology of acute promyelocytic leukemia. Cancer Treat Res 1999;99:75–124.
[32] Shao W, Rosenauer A, Mann K, Chang CP, Rachez C, Freedman LP, et al. Ligand-inducible interaction of the DRIP/TRAP co-activator complex with retinoid receptors in retinoic acid-sensitive and -resistant acute promyelocytic leukemia cells. Blood 2000;96:2233–9.
[33] Imaizumi M, Breitman TR. Retinoic acid-induced differentiation of the human promyelocytic leukemia cell line, HL-60, and fresh human leukemia cells in primary culture: a model for differentiation inducing therapy of leukemia. Eur J Haematol 1987;38:289–302.
[34] Taimi M, Breitman TR. Growth, differentiation, and death of retinoic acid-treated human acute promyelocytic leukemia NB4 cells. Exp Cell Res 1997;230:69–75.
[35] Chambon P. A decade of molecular biology of retinoic acid receptors. FASEB J 1996;10:940–54.
[36] Fanelli M, Minucci S, Gelmetti V, Nervi C, Gambacorti-Passerini C, Pelicci PG. Constitutive degradation of PML/RARα through the proteasome pathway mediates retinoic acid resistance. Blood 1999;93:1477–81.
[37] Benoit G, Altucci L, Flexor M, Ruchaud S, Lillehaug J, Raffelsberger W, et al. RAR-independent RXR signaling induces t(15;17) leukemia cell maturation. EMBO J 1999;18:7011–8.
[38] Takahashi N, Breitman TR. Covalent modification of proteins by ligands of steroid hormone receptors. Proc Natl Acad Sci USA 1992;89:10807–11.
[39] Yoshinari M, Imaizumi M, Sato A, Minegishi M, Fujii K, Suzuki H. G-CSF induces apoptosis of a human acute promyelocytic leukemia cell line, UF-1: possible involvement of Stat3 activation and altered Bax expression. Tohoku J Exp Med 1999;189:71–82.
[40] Rego EM, Wang ZG, Peruzzi D, He LZ, Cordon-Cardo C, Pandolfi PP. Role of promyelocytic leukemia (PML) protein in tumor suppression. J Exp Med 2001;193:521–9.

0021-972X/04/$15.00/0
Printed in U.S.A.

The Journal of Clinical Endocrinology & Metabolism 89(8):4113–4118

doi: 10.1210/jc.2004-0069

Nur-Related Factor 1 and Nerve Growth Factor-Induced Clone B in Human Adrenal Cortex and Its Disorders

LIANGYING LU, TAKASHI SUZUKI, YOSUKE YOSHIKAWA, OSAMU MURAKAMI, YASUHIRO MIKI, TAKUYA MORIYA, MARY H. BASSETT, WILLIAM E. RAINEY, YUTAKA HAYASHI, AND HIRONOBU SASANO

Departments of Pathology (L.L., T.S., Y.Y., Y.M., T.M., H.S.), Pediatric Surgery (L.L., Y.H.), and Second Department of Internal Medicine (O.M.), Tohoku University School of Medicine, 980-8575 Sendai, Japan; and Division of Reproductive Endocrinology (M.H.B., W.E.R.), University of Texas Southwestern Medical Center, Dallas, Texas 75390-9032

Nerve growth factor-induced clone B (NGFI-B; NR4A1) and Nur-related factor 1 (Nurr1; NR4A2) are members of NGFI-B family of orphan receptors. We recently demonstrated induction of CYP11B2 (aldosterone synthase) by Nurr1 and NGFI-B, suggesting possible important roles of these transcriptional factors in the regulation of adrenocortical steroidogenesis. Therefore, we immunolocalized Nurr1 and NGFI-B in various human adrenal specimens to study their biological significance. In nonpathological adrenal glands (n = 25), Nurr1 and NGFI-B immunoreactivities were detected at high levels in the fetal definitive zone or postnatal zona glomerulosa. NGFI-B immunoreactivity was increased according to development in the zona fasciculata, reaching a level similar to that in the zona glomerulosa in adult adrenal cortex. In adrenocortical neoplasms (n = 44), Nurr1 immunoreactivity was higher in aldosteronoma than in Cushing's adenoma or adrenocortical carcinoma. NGFI-B immunoreactivity was also higher in aldosteronoma than in adrenocortical carcinoma, but was not significantly different among the types of adenoma. Both Nurr1 and NGFI-B mRNA expressions were correlated with their immunoreactivities in adrenocortical neoplasms (n = 23), and mRNA expression of Nurr1 was significantly ($P < 0.0001$) associated with that of CYP11B2. These results suggest that the expression of Nurr1 and NGFI-B plays an important role in human adrenal cortex and its neoplasms, including possible regulation of steroidogenesis. (*J Clin Endocrinol Metab* 89: 4113–4118, 2004)

HUMAN ADRENAL CORTEX is composed of three distinct zones, *i.e.* the zonae glomerulosa, fasciculata, and reticularis. These three zones produce distinct steroid hormones, such as aldosterone in the zona glomerulosa, cortisol in the zona fasciculata, and dehydroepiandrosterone and dehydroepiandrosterone sulfate in the zona reticularis (1). This functional zonation results from the zone-specific expression of steroidogenic enzymes (2). It is also well known that adrenocortical neoplasms excessively produce various corticosteroids and are generally associated with an abnormal expression of steroidogenic enzymes (3–5). Therefore, it is very important to examine the possible regulation of adrenocortical steroidogenesis to obtain a better understanding of functions of the human adrenal cortex and its disorders.

Nerve growth factor-induced clone B (NGFI-B; NR4A1) and Nurr1 (Nur-related factor 1; NR4A2) belong to a NGFI-B family of nuclear hormone receptors as well as neuron-derived orphan receptor 1 (NR4A3) (6). These nuclear receptors activate transcription by binding to the NGFI-B-responsive elements (NBREs) located in the promoter region of target genes (7, 8) and regulate various cellular functions, such as the differentiation of neural cells (9, 10), the apoptosis of T lymphocytes in the thymus (11), and the modulation of retinoic acid signal transduction (12). The expression of Nurr1 and NGFI-B has been previously detected in murine adrenal glands (13). Very recently, we demonstrated that the human CYP11B2 (aldosterone synthase) gene, which is a key enzyme of aldosterone production, contains NBRE in the promoter region, and its expression was markedly induced by Nurr1 or NGFI-B (14). These *in vitro* data suggest important roles for Nurr1 and NGFI-B in the human adrenal cortex, including the regulation of steroidogenesis. However, a detailed examination of the expression of these nuclear receptors has not been reported in the human adrenal gland and its disorders. Therefore, after the previous *in vitro* study (14), we immunolocalized Nurr1 and NGFI-B in nonpathological and pathological specimens of human adrenal cortex. In addition, we examined mRNA expression of Nurr1 and NGFI-B in adrenocortical neoplasms using real-time RT-PCR and examined the correlation with CYP11B2 mRNA expression.

Materials and Methods

Human adrenal specimens

Sixty-nine human adrenal specimens were examined in this study. Twenty-five specimens of nonpathological adrenal glands were obtained from autopsy files (11–36 wk gestation and 1 d to 68 yr of age) from Tohoku University Hospital (Sendai, Japan). Forty-four cases of adrenocortical tumors (14 aldosteromas, 10 Cushing's adenomas, 10 nonfunctioning adenomas with no clinical hormonal abnormalities, and 10 adrenocortical carcinomas) were retrieved from the surgical pathology files of Tohoku University Hospital. Adrenocortical carcinomas were histologically diagnosed based on the criteria of Weiss (15). These

Abbreviations: GAPDH, Glyceraldehyde-3-phosphate dehydrogenase; 3βHSD2, 3β-hydroxysteroid dehydrogenase type 2; NBRE, nerve growth factor-induced clone B-responsive element; NGFI-B, nerve growth factor-induced clone B; Nurr1, Nur-related factor 1.

JCEM is published monthly by The Endocrine Society (http://www.endo-society.org), the foremost professional society serving the endocrine community.

specimens were fixed in 10% formalin for 24–48 h at room temperature and embedded in paraffin wax.

Twenty-three cases of adrenocortical neoplasms were also available for real-time RT-PCR analysis (eight aldosteronomas, six Cushing's adenomas, six nonfunctioning adenomas, and three adrenocortical carcinomas). Specimens for RNA isolation were snap-frozen and stored at −80 C.

Research protocols for this study were approved by the ethics committee at Tohoku University School of Medicine.

Immunohistochemistry

Rabbit polyclonal antibodies for Nurr1 (sc-991) and NGFI-B (1600045) were purchased from Santa Cruz Biotechnology, Inc. (Santa Cruz, CA), and Geneka Biotechnology (Montréal, Canada), respectively. Utilization of these antibodies for immunohistochemistry has been reported previously (14).

Immunohistochemical analysis was performed employing the streptavidin-biotin amplification method using a Histofine Kit (Nichirei, Tokyo, Japan). Antigen retrieval was performed by heating the slides in an autoclave at 120 C for 5 min in citric acid buffer (2 mM citric acid and 9 mM trisodium citrate dehydrate, pH 6.0). The dilutions of the primary antibodies used in this study were: Nurr1, 1:250; and NGFI-B, 1:200. The antigen-antibody complex was visualized with 3,3′-diaminobenzidine solution [1 mM 3,3′-diaminobenzidine, 50 mM Tris-HCl buffer (pH 7.6), and 0.006% H_2O_2] and counterstained with hematoxylin. Immunohistochemical preabsorption tests for Nurr1 and NGFI-B were performed for negative controls of immunohistochemistry. Normal rabbit IgG was also used in place of the primary antibodies as a negative control.

Evaluation of immunoreactivity

After completely reviewing immunohistochemical sections, relative immunoreactivity for Nurr1 and NGFI-B in each zone of adrenocortex was evaluated by an H scoring system, as described by McCarty *et al.* (16) with some modifications (17). Briefly, adrenocortical cells were counted in each zone, and H-scores were subsequently generated by adding together 2 × the percentage of strongly stained nuclei, 1 × the percentage of weakly stained nuclei, and 0 × the percentage of negative nuclei, giving a possible range of 0–200. The H scores were independently and blindly evaluated by three of the authors (T.S., T.M., and H.S.) to obtain immunohistochemical data objectively, and the mean of the three values was used for analysis. The adrenals were classified into the following age groups in this study: 11–36wk gestation (n = 5), 1 d to 5 months of age (n = 4), 11 months to 8 yr of age (n = 5), 10–18 yr of age (n = 5), and 27–68 yr of age (n = 6). The relative immunoreactivity of tumor cells was also evaluated by H-scoring system described above. Statistical significance was evaluated using a Bonferroni test, and $P < 0.05$ was considered significant.

Real-time RT-PCR

Total RNA was carefully extracted from 23 specimens of adrenocortical neoplasms with guanidinium thiocyanate, followed by ultracentrifugation in cesium chloride. An RT kit (SuperScript II Preamplification System, Invitrogen Life Technologies, Inc., Grand Island, NY) was used in the synthesis of cDNA.

The Light Cycler System (Roche, Mannheim, Germany) was used to semiquantify the mRNA levels of Nurr1, NGFI-B, and CYP11B2 in 22 adrenocortical neoplasms by real-time PCR (18). Settings for the PCR thermal profile were: initial denaturation at 95 C for 1 min, followed by 40 amplification cycles of 95 C for 0 sec, annealing at 66 C (Nurr1, NGFI-B, and glyceraldehyde-3-phosphate dehydrogenase (GAPDH)) or 60 C (CYP11B2) for 15 sec, and elongation at 72 C for 15 sec. The primer sequences used in this study are as follows: Nurr1: forward, 5′-AACCCTGACTATCAAATGAGTG-3′; reverse, 5′-CAATGCAGGAGAAGGCAGAAAT-3′ (19); NGFI-B, forward, 5′-TCTGCTCAGGCCTGGTGCTAC-3′; reverse, 5′-GGCACCAAGTCCTCCAGCTTG-3′ (20); CYP11B2: forward, 5′-TCCTGCTCTTCTTGCATCTGG-3′; reverse, 5′-TTTGCCCTGCAAATGGTTG-3′ (21); and GAPDH: forward, 5′-TGAACGG-

TABLE 1A. Relative immunoreactivity of Nurr1 in nonpathological human adrenal cortex

Age group (no. of cases)	Fetal type		Adult type		
	Definitive zone	Fetal zone	Glomerulosa	Fasciculata	Reticularis
Fetus					
11–36 wk gestation (n = 5)	151 ± 19.8	26.0 ± 4.74[a]			
After birth					
1 d–5 months (n = 4)	153 ± 19.0	28.7 ± 9.82[a]			
11 months–8 yr (n = 5)			132 ± 8.95	58.8 ± 16.5[b]	15.3 ± 7.76[b,c]
10–18 yr (n = 5)			150 ± 14.8	69.8 ± 17.9[b]	7.20 ± 3.43[b,c]
27–68 yr (n = 6)			147 ± 16.9	77.3 ± 13.2[b]	13.8 ± 6.65[b,c]

The relative immunoreactivity of each zone in the adrenal cortex was evaluated by the H scoring system (0–200). Data are the mean ± SEM.
[a] $P < 0.001$ *vs.* definitive zone.
[b] $P < 0.001$ *vs.* zona glomerulosa.
[c] $P < 0.001$ *vs.* zona fasciculata.

TABLE 1B. Relative immunoreactivity of NGFI-B in nonpathological human adrenal cortex

Age group (no. of cases)	Fetal type		Adult type		
	Definitive zone	Fetal zone	Glomerulosa	Fasciculata	Reticularis
Fetus					
11–36 wk gestation (n = 5)	122 ± 12.6	24.2 ± 3.61[a]			
After birth					
1 d–5 months (n = 4)	125 ± 24.3	20.8 ± 5.83[a]			
11 months–8 yr (n = 5)			143 ± 12.5	53.0 ± 16.7[b]	16.7 ± 5.54[b]
10–18 yr (n = 5)			147 ± 12.4	113 ± 8.09[c,d]	12.7 ± 2.40[b,e]
27–68 yr (n = 6)			167 ± 8.87	132 ± 7.94[c,f]	24.8 ± 12.0[b,e]

The relative immunoreactivity of each zone in the adrenocortex was evaluated by the H scoring system (0–200). Data are the mean ± SEM.
[a] $P < 0.001$ *vs.* definitive zone.
[b] $P < 0.001$ *vs.* zona glomerulosa.
[c] $P < 0.05$ *vs.* zona glomerulosa.
[d] $P < 0.05$ *vs.* age 11 months–8 yr.
[e] $P < 0.001$ *vs.* zona fasciculata.
[f] $P < 0.01$ *vs.* age 11 months–8 yr.

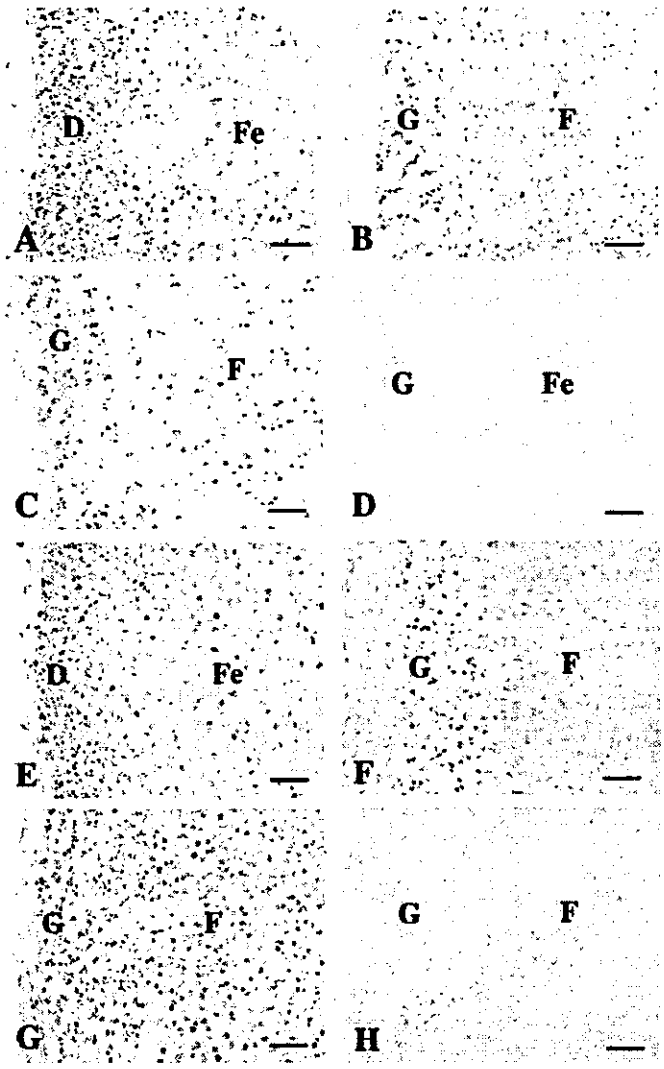

FIG. 1. Immunohistochemistry for Nurr1 (A–D) and NGFI-B (E–H) in the adrenal cortex. A, Immunoreactivity for Nurr1 was detected at a high level in the nuclei of cortical cells in the definitive zone (D; 11 wk gestation). Fe, Fetal zone. B and C, Nurr1 immunoreactivity was detected at a high level in the zona glomerulosa (G; B, 5 yr of age; C, 49 yr of age). F, Zona fasciculata. D, Immunohistochemical preabsorption test for Nurr1 showed no specific immunoreactivity. E, NGFI-B immunoreactivity was detected at a high level in the definitive zone (14 wk gestation). F, At 11 months of age, immunoreactivity for NGFI-B was high in the zona glomerulosa, but low in the zona fasciculata. G, NGFI-B immunoreactivity was high in both zonae glomerulosa and fasciculata in the adrenocortex at 28 yr of age. H, Immunohistochemical preabsorption test for NGFI-B. No specific immunoreactivity was detected. *Bar*, 50 μm.

GAAGCTCACTGG-3′; and reverse, 5′-TCCACCACCCTGTTGCTGTA-3′ (22). To verify amplification of the correct sequences, PCR products were purified and subjected to direct sequencing. Nonpathological adrenal tissues were used as positive controls for Nurr1, NGFI-B, and CYP11B2. Negative control experiments lacked cDNA substrate to check for the possibility of exogenous contaminant DNA, and no amplified products were detected under these conditions. The mRNA level for Nurr1, NGFI-B, and CYP11B2 in each case has been summarized as a ratio of GAPDH, and subsequently evaluated as a ratio (percentage) compared with that in the positive controls (nonpathological adrenal glands = 100%).

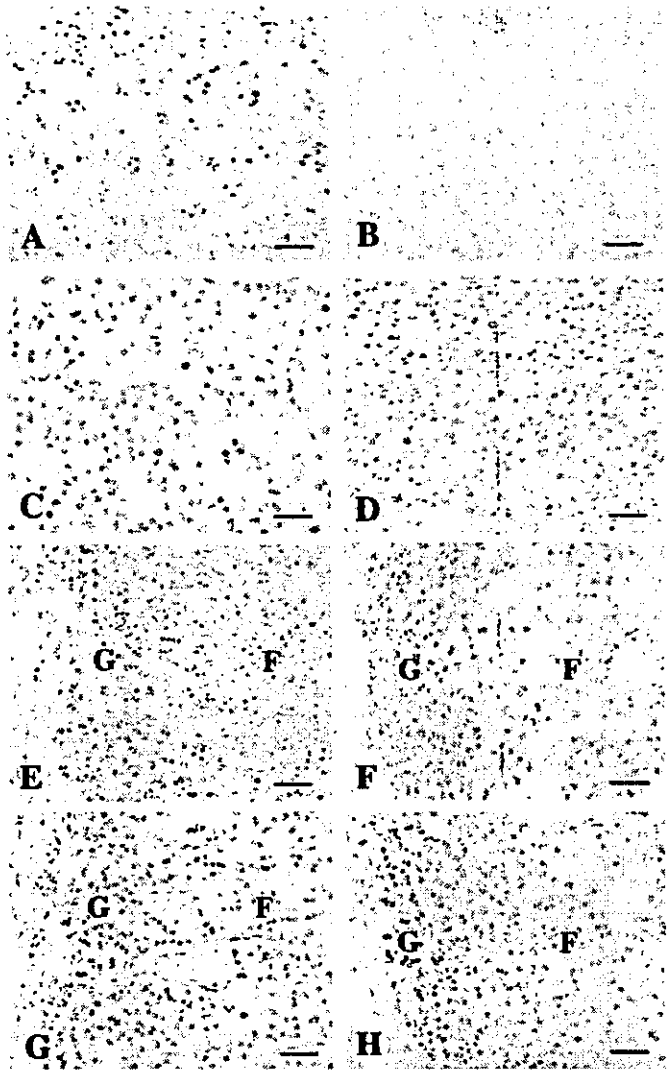

FIG. 2. Immunohistochemistry for Nurr1 and NGFI-B in adrenocortical adenoma (A–D) and its attached nonneoplastic adrenal cortex (E–H). A–D, Nurr1 immunoreactivity was detected at a high level in the nuclei of tumor cells in aldosteronoma (A), whereas a great majority of tumor cells were negative for Nurr1 in Cushing's adenoma (B). NGFI-B immunoreactivity was detected at a high level in aldosteronoma (C; same case as in A) or Cushing's adenoma (D; same case as in B). E–H, Nurr1 (E and F) and NGFI-B (G and H) immunoreactivities were not significantly different in the attached nonneoplastic adrenocortex regardless of the type of adenoma. E–H were taken from the same slide as A–D, respectively. *Bar*, 50 μm.

Results

Nonpathological adrenal cortex

Results for Nurr1 immunoreactivity in nonpathological human adrenocortex are summarized in Table 1A. Nurr1 immunoreactivity was detected in the nuclei of cortical cells, and its relative immunoreactivity was significantly ($P < 0.0001$) higher in the definitive zone (151 ± 19.8) than in the fetal zone (26.0 ± 4.74) of the fetal adrenal (Fig. 1A). At 11 months to 8 yr of age, immunoreactivity for Nurr1 was significantly higher in the zona glomerulosa (132 ± 8.95) than in the zonae fasciculata (58.8 ± 16. 5) and reticularis (15.3 ±

7.76; $P < 0.0001$, respectively). Nurr1 immunoreactivity in each zone was not significantly changed among the age groups examined (11 months to 8 yr, 10–18 yr, and 24–62 yr; Fig. 1, B and C).

Results for NGFI-B immunoreactivity in nonpathological adrenal cortex are summarized in Table 1B. NGFI-B immunoreactivity was detected in the nuclei of cortical cells, and its relative immunoreactivity was significantly ($P < 0.0001$) higher in the definitive zone (122 ± 12.6) than in the fetal zone (24.2 ± 3.61; Fig. 1E). At 11 months to 8 yr of age, NGFI-B immunoreactivity was significantly higher in the zona glomerulosa (143 ± 12.5) than in the zonae fasciculata (53.0 ± 16.7) and reticularis (16.7 ± 5.54; $P < 0.0001$, respectively; Fig. 1F). Immunoreactivity for NGFI-B in the zona fasciculata was significantly increased in adolescent and adult age groups (10–18 yr, 113 ± 8.09; 27–68 yr, 132 ± 7.94) compared with that the 11 months to 8 yr of age group ($P < 0.05$, and $P < 0.01$, respectively; Fig. 1G), whereas NGFI-B immunoreactivity in the zonae glomerulosa and reticularis was not significantly changed.

Adrenocortical tumor

The results for Nurr1 and NGFI-B immunoreactivity in adrenocortical tumors are summarized in Table 2A. Nurr1 relative immunoreactivity was significantly higher in aldosteronoma (121 ± 9.91; Fig. 2A) than in Cushing's adenoma (62.1 ± 12.2; Fig. 2B) and adrenocortical carcinoma (60.0 ± 19.0; $P < 0.001$, respectively). NGFI-B immunoreactivity was also higher ($P < 0.05$) in aldosteronoma (122 ± 14.3; Fig. 2C) than in adrenocortical carcinoma (76.4 ± 13.6), but its difference among the types of adrenocortical adenoma did not reach statistical significance (Fig. 2D).

The results for Nurr1 and NGFI-B immunoreactivity in attached nonneoplastic adrenal cortex of adenoma are summarized in Table 2, B and C. The relative immunoreactivity of Nurr1 and NGFI-B in attached nonneoplastic adrenocortex of adenoma was not significantly changed regardless of the type of adenoma examined (Fig. 2, E–H).

mRNA expression of Nurr1, NGFI-B, and CYP11B2 in adrenocortical adenoma

mRNA expression for Nurr1, NGFI-B, and CYP11B2 was detected as a specific single band (352, 358, and 121 bp, respectively) and was semiquantified by real-time RT-PCR. mRNA expression of Nurr1 and NGFI-B was detected in all adrenocortical adenomas examined, and the range of mRNA levels was 0.160–354% for Nurr1 and 12.0–223% for NGFI-B (nonpathological adrenal glands = 100%, respectively). As shown in Fig, 3, A and B, the mRNA levels of Nurr1 and NGFI-B were significantly correlated with the relative immunoreactivity (for Nurr1: $r = 0.896$; $P < 0.0001$; for NGFI-B: $r = 0.787$; $P < 0.0001$). mRNA expression of Nurr1 was significantly associated with that of CYP11B2 ($r = 0.765$; $P < 0.0001$; Fig. 3C), whereas no significant association was detected between NGFI-B and CYP11B2 mRNA levels ($r = 0.213$; $P = 0.3301$; Fig. 3D).

TABLE 2A. Relative immunoreactivity of Nurr1 and NGFI-B in adrenocortical tumors

Type of tumor (no. of cases)	Nurr1	NGFI-B
Aldosteronoma (n = 14)	121 ± 9.91	122 ± 14.3
Cushing's adenoma (n = 10)	62.1 ± 12.2[a]	105 ± 13.0
Nonfunctioning adenoma (n = 10)	91.8 ± 12.6	90.0 ± 19.6
Carcinoma (n = 10)	60.0 ± 19.0[a]	76.4 ± 13.6[b]

The relative immunoreactivity was evaluated by the H scoring system in each case (0–200). Data are the mean ± SEM.
[a] $P < 0.01$ *vs.* aldosteronoma.
[b] $P < 0.05$ *vs.* aldosteronoma.

Discussion

Aldosterone is produced in the zona glomerulosa of the adrenal cortex through an interaction of several steroidogenic enzymes, including P450 side-chain cleavage (CYP11A), 3β-hydroxysteroid dehydrogenase type 2 (3βHSD2), CYP21, and CYP11B2. Among these enzymes, CYP11B2 is a specific enzyme for aldosterone biosynthesis, and it is expressed exclusively in the zona glomerulosa (23).

TABLE 2B. Relative immunoreactivity of Nurr1 in the adjacent nonneoplastic adrenal cortex of adenomas

Type of adenoma (no. of cases)	Glomerulosa	Fasciculata	Reticularis
Aldosteronoma (n = 14)	124 ± 10.8	72.4 ± 9.62[a]	17.1 ± 3.94[a,b]
Cushing's adenoma (n = 10)	143 ± 10.8	88.6 ± 12.5[a]	24.2 ± 6.21[a,b]
Nonfunctioning adenoma (n = 10)	124 ± 11.3	60.9 ± 9.61[a]	9.38 ± 4.26[a,b]
Nonpathological adrenal (27–68 yr; n = 6)[c]	147 ± 16.9	77.3 ± 13.2[a]	13.8 ± 6.65[a,b]

The relative immunoreactivity of each zone in the adrenal was evaluated by the H scoring system (0–200). Data are the mean ± SEM.
[a] $P < 0.001$ *vs.* zona glomerulosa.
[b] $P < 0.001$ *vs.* zona fasciculata.
[c] Data were taken from Table 1A.

TABLE 2C. Relative immunoreactivity of NGFI-B in the attached nonneoplastic adrenal cortex of adenomas

Type of adenoma (no. of cases)	Glomerulosa	Fasciculata	Reticularis
Aldosteronoma (n = 14)	149 ± 8.97	111 ± 12.1[a]	22.6 ± 12.0[b]
Cushing's adenoma (n = 10)	151 ± 11.3	119 ± 10.5[a]	22.4 ± 4.30[b]
Nonfunctioning adenoma (n = 10)	143 ± 7.4	109 ± 9.80[a]	25.8 ± 4.46[b]
Nonpathological adrenal (27–68 yr; n = 6)[c]	167 ± 8.87	132 ± 7.94[a]	24.8 ± 12.0[b]

The relative immunoreactivity of each zone in the adrenal was evaluated by the H scoring system (0–200). Data are the mean ± SEM.
[a] $P < 0.05$ *vs.* zona glomerulosa.
[b] $P < 0.001$ *vs.* zona glomerulosa. $P < 0.001$ *vs.* zona fasciculata.
[c] Data were taken from Table 1B.

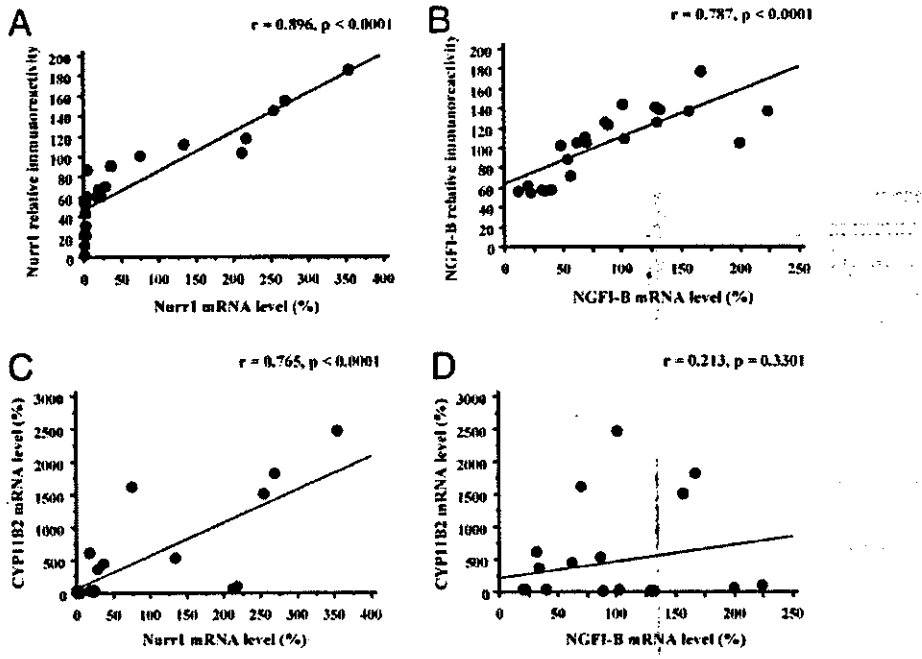

FIG. 3. A and B, Association between the mRNA level and the relative immunoreactivity of Nurr1 (A) or NGFI-B (B) in 23 cases of adrenocortical adenomas. Significant positive associations were detected (for Nurr1: r = 0.896; $P < 0.0001$; for NGFI-B: r = 0.787; $P < 0.0001$). C and D, Association between the mRNA level of Nurr1 (C) or NGFI-B (D) and that of CYP11B2 in 23 adrenocortical adenomas. CYP11B2 mRNA was significantly correlated with Nurr1 mRNA (r = 0.765; $P < 0.0001$), but not with NGFI-B mRNA (r = 0.213; $P = 0.3301$).

Very recently, Bassett *et al.* (14) demonstrated that the CYP11B2 gene has two functional NBREs in the promoter region and was markedly up-regulated by Nurr1 and NGFI-B. In this study Nurr1 immunoreactivity was present at a high level in the zona glomerulosa or aldosteronoma, and mRNA expression of Nurr1 was significantly correlated with that of CYP11B2 in adrenocortical neoplasms. Therefore, it is suggested that Nurr1 expression plays an important role in aldosterone production through the induction of CYP11B2 in the zona glomerulosa of adrenal cortex or aldosteronoma. However, it is also true that Nurr1 immunoreactivity was detected at low levels in the zona fasciculata or adrenocortical neoplasms in addition to aldosteronoma in this study. Activation of Nurr1 depends on two so-called activation functions (AF1 and AF2), located at the N- or C-terminal regions, and it was partly regulated by the phosphorylation (24). Therefore, posttranslational modifications of Nurr1 are also considered to play some role in the zone-specific expression of CYP11B2 in the adrenal gland. In adrenocortical adenomas expressed Nurr1 mRNA at low levels, relative immunoreactivity of Nurr1 was variably detected (Fig. 3A). In these cases, evaluation of Nurr1 mRNA in tumor tissues may be reflected by heterogeneous expression of Nurr1 in neoplastic cells and/or amounts of stroma within the samples.

NGFI-B immunoreactivity was detected at high levels in the zonae glomerulosa and fasciculata in the nonpathological adrenal gland and in various types of adrenocortical adenoma. The zona fasciculata is mainly involved in cortisol production, and CYP11A, 3βHSD2, CYP17, CYP21, and CYP11B1 (11β-hydroxylase) are expressed in this zone. Previous studies demonstrated that human and mouse CYP21 gene promoters contain NBREs, and induction of CYP21 transcription by NGFI-B has been proposed (20, 25). In addition, Bassett *et al.* (26) recently demonstrated that 3βHSD2 contains an NBRE in the promoter region and was significantly up-regulated by NGFI-B. On the other hand, NGFI-B had no effect on the induction of CYP11B1 (14) and CYP17 (26), which are not expressed in the zona glomerulosa (2, 23, 27). Therefore, NGFI-B may be partly involved in aldosterone and/or cortisol production through the regulation of some related enzyme expressions in the adrenal cortex and its neoplasms.

In fetal adrenal glands, immunoreactivity of steroidogenic enzymes is known to become generally discernible after 23 wk gestation in the definitive zone (28), and the definitive zone is considered to become steroidogenically active in the late phase of pregnancy (29). However, Nurr1 and NGFI-B immunoreactivities were detected in the definitive zone in all fetal adrenals examined (from 11–36 wk gestational) in our study. Therefore, the expression of Nurr1 and NGFI-B is postulated to occur before the expression of steroidogenic enzymes in the definitive zone in the fetal adrenals. Rainey *et al.* (30) reported that NGFI-B mRNA expression was very low in the fetal adrenal gland (15–20 wk gestation) compared with that in the adult adrenal by microarray and Northern analyses. These data are not necessarily consistent with our present results, but may be due to the different gestational ages examined or the different examination methods used. In addition, the fact that microarray and/or Northern analysis required a whole adrenal specimen may contribute to this difference from the present immunohistochemical study, because the definitive zone is markedly thin and much smaller in volume than the fetal zone in human adrenal.

Autonomous neoplastic production of cortisol in Cushing's adenoma or at least some nonfunctioning adenoma patients results in adrenocortical atrophy with suppression of steroidogenic enzyme in the zonae fasciculata/reticularis of the adjacent nonneoplastic adrenocortex through inhibition of ACTH secretion. In addition, the expression of steroidogenic enzymes is markedly decreased, except for CYP21, in the zona glomerulosa of the adjacent nonneoplas-

tic adrenocortex in patients with aldosteronoma (2, 31). Previous *in vitro* studies demonstrated that Nurr1 and/or NGFI-B were rapidly induced by various factors, including ACTH (32) and angiotensin II (14). However, unexpectedly, Nurr1 and NGFI-B immunoreactivities in the attached nonneoplastic adrenal cortex of adenoma were not significantly different from those in the nonpathological adrenal cortex in our study. It is difficult to explain the mechanisms of these findings, but Davis and Lau (32) reported that NGFI-B isolated from ACTH-stimulated Y-1 cells was hypophosphorylated at serine 354 and significantly bound to its responsive element, whereas NGFI-B present in the unstimulated cells did not. The expression of Nurr1 or NGFI-B was generally considered to be regulated by multiple pathways, and the transcriptional activity is intricately modulated by phosphorylation (24). Therefore, a decrement in steroidogenesis in the attached nonneoplastic adrenal cortex of an adenoma may be partly due to the changes in posttranslational modifications of Nurr1 and/or NGFI-B. Additional examinations are required to clarify this hypothesis.

Acknowledgments

We appreciate the assistance of Ms. Chika Kaneko and Mr. Katsuhiko Ono (Department of Pathology, Tohoku University School of Medicine, respectively) for their skillful technical assistance.

Received January 14, 2004. Accepted May 5, 2004.

Address all correspondence and requests for reprints to: Dr. Takashi Suzuki, Department of Pathology, Tohoku University School of Medicine, 2-1 Seiryo-machi, Aoba-ku, Sendai 980-8575, Japan. E-mail: t-suzuki@patholo2.med.tohoku.ac.jp.

This work was supported in part by NIH Grant DK-43140 (to W.E.R.).

References

1. **Neville AM, O'Hare MJ** 1982 Functional activity of the adrenal cortex. In: The human adrenal cortex. New York: Springer-Verlag; 68–98
2. **Sasano H** 1994 Localization of steroidogenic enzymes in adrenal cortex and its disorders. Endocr J 41:471–482
3. **Ogishima T, Shibata H, Shimada H, Mitani F, Suzuki H, Saruta T, Ishimura Y** 1991 Aldosterone synthase cytochrome P-450 expressed in the adrenals of patients with primary aldosteronism. J Biol Chem 266:10731–10734
4. **Ogo A, Haji M, Ohashi M, Nawata H** 1991 Markedly increased expression of cytochrome P-450 17α-hydroxylase (P-450c17) mRNA in adrenocortical adenomas from patients with Cushing's syndrome. Mol Cell Endocrinol 80:83–89
5. **Suzuki T, Sasano H, Sawai T, Tsunoda K, Nisikawa T, Abe K, Yoshinaga K, Nagura H** 1992 Small adrenocortical tumors without apparent clinical endocrine abnormalities. Immunolocalization of steroidogenic enzymes. Pathol Res Pract 188:883–889
6. **Giguere V** 1999 Orphan nuclear receptors: from gene to function. Endocr Rev 20:689–725
7. **Davis IJ, Hazel TG, Lau LF** 1991 Transcriptional activation by Nur77, a growth factor-inducible member of the steroid hormone receptor superfamily. Mol Endocrinol 5:854–859
8. **Wilson TE, Fahrner TJ, Johnston M, Milbrandt J** 1991 Identification of the DNA binding site for NGFI-B by genetic selection in yeast. Science 252:1296–1300
9. **Saucedo-Cardenas O, Quintana-Hau JD, Le WD, Smidt MP, Cox JJ, De Mayo F, Burbach JP, Conneely OM** 1998 Nurr1 is essential for the induction of the dopaminergic phenotype and the survival of ventral mesencephalic late dopaminergic precursor neurons. Proc Natl Acad Sci USA 95:4013–4018
10. **Milbrandt J** 1998 Nerve growth factor induces a gene homologous to the glucocorticoid receptor gene. Neuron 1:183–188
11. **Lee SL, Wesselschmidt RL, Linette GP, Kanagawa O, Russell JH, Milbrandt J** 1995 Unimpaired thymic and peripheral T cell death in mice lacking the nuclear receptor NGFI-B (Nur77). Science 269:532–535
12. **Perlmann T, Jansson L** 1995 A novel pathway for vitamin A signaling mediated by RXR heterodimerization with NGFI-B and NURR1. Genes Dev 9:769–782
13. **Davis IJ, Lau LF** 1994 Endocrine and neurogenic regulation of the orphan nuclear receptors Nur77 and Nurr-1 in the adrenal glands. Mol Cell Biol 14:3469–3483
14. **Bassett M, Suzuki T, Sasano H, White PC, Rainey WE** 2004 A role for the NGFIB family of transactivation factors in adrenal aldosterone production. Mol Endocrinol 18:279–290
15. **Weiss LM** 1984 Comparative histologic study of 43 metastasizing and nonmetastasizing adrenocortical tumors. Am J Surg Pathol 8:163–169
16. **McCarty Jr KS, Miller LS, Cox EB, Konrath J, McCarty KS Sr** 1985 Estrogen receptor analyses. Correlation of biochemical and immunohistochemical methods using monoclonal antireceptor antibodies. Arch Pathol Lab Med 109:716–721
17. **Suzuki T, Takahashi K, Darnel AD, Moriya T, Murakami O, Narasaka T, Takeyama J, Sasano H** 2000 COUP-TFII in the human adrenal cortex and its disorders. J Clin Endocrinol Metab 85:2752–2757
18. **Dumoulin FL, Nischalke HD, Leifeld L, von dem Bussche A, Rockstroh JK, Sauerbruch T, Spengler U** 2000 Semi-quantification of human C-C chemokine mRNAs with reverse transcription/real-time PCR using multi-specific standards. J Immunol Methods 241:109–119
19. **Maruyama K, Tsukada T, Bandoh S, Sasaki K, Ohkura N, Yamaguchi K** 1995 Expression of NOR-1 and its closely related members of the steroid/thyroid hormone receptor superfamily in human neuroblastoma cell lines. Cancer Lett 96:117–122
20. **Wilson TE, Mouw AR, Weaver CA, Milbrandt J, Parker KL** 1993 The orphan nuclear receptor NGFI-B regulates expression of the gene encoding steroid 21-hydroxylase. Mol Cell Biol 13:861–868
21. **Yoshimura M, Nakamura S, Ito T, Nakayama M, Harada E, Mizuno Y, Sakamoto T, Yamamuro M, Saito Y, Nakao K, Yasue H, Ogawa H** 2002 Expression of aldosterone synthase gene in failing human heart: quantitative analysis using modified real-time polymerase chain reaction. J Clin Endocrinol Metab 87:3936–3940
22. **Suzuki T, Nakata T, Miki Y, Kaneko C, Moriya T, Ishida T, Akinaga S, Hirakawa H, Kimura M, Sasano H** 2003 Estrogen sulfotransferase and steroid sulfatase in human breast carcinoma. Cancer Res 63:2762–2770
23. **Rainey WE** 1999 Adrenal zonation: clues from 11β-hydroxylase and aldosterone synthase. Mol Cell Endocrinol 151:151–160
24. **Nordzell M, Aarnisalo P, Benoit G, Castro DS, Perlmann T** 2004 Defining an N-terminal activation domain of the orphan nuclear receptor Nurr1. Biochem Biophys Res Commun 313:205–211
25. **Chang SF, Chung BC** 1995 Difference in transcriptional activity of two homologous CYP21A genes. Mol Endocrinol 9:1330–1336
26. **Bassett MH, Jimemez PT, Carr BR, Rainey WE,** Transcriptional regulation of 3β-hydroxysteroid dehydrogenase type 2 (3βHSD2) by the transcription factor NGFIB (NR4A1). Proc of the 84th Annual Meeting of The Endocrine Society, San Francisco, CA, 2002, p 342 (Abstract P2–86)
27. **Suzuki T, Sasano H, Takeyama J, Kaneko C, Freije WA, Carr BR, Rainey WE** 2000 Developmental changes in steroidogenic enzymes in human postnatal adrenal cortex: immunohistochemical studies. Clin Endocrinol (Oxf) 53: 739–747
28. **Narasaka T, Suzuki T, Moriya T, Sasano H** 2001 Temporal and spatial distribution of corticosteroidogenic enzymes immunoreactivity in developing human adrenal. Mol Cell Endocrinol 174:111–120
29. **Mesiano S, Jaffe RB** 1997 Developmental and functional biology of the primate fetal adrenal cortex. Endocr Rev 18:378–403
30. **Rainey WE, Carr BR, Wang ZN, Parker Jr CR** 2001 Gene profiling of human fetal and adult adrenals. J Endocrinol 171:209–215
31. **Sasano H, White PC, New MI, Sasano N** 1988 Immunohistochemical localization of cytochrome P-450C21 in human adrenal cortex and its relation to endocrine function. Hum Pathol 19:181–185
32. **Davis IJ, Lau LF** 1994 Endocrine and neurogenic regulation of the orphan nuclear receptors Nur77 and Nurr-1 in the adrenal glands. Mol Cell Biol 14:3469–3483

JCEM is published monthly by The Endocrine Society (http://www.endo-society.org), the foremost professional society serving the endocrine community.

Journal of Pediatric Surgery (2005) 40, 359–363

ELSEVIER

Journal of
Pediatric
Surgery

www.elsevier.com/locate/jpedsurg

Profile of neuroblastoma detected by mass screening, resected after observation without treatment: results of the Wait and See pilot study

Takaharu Oue[a,*], Masami Inoue[b], Akihiro Yoneda[c], Akio Kubota[c], Hiroomi Okuyama[c], Hisayoshi Kawahara[c], Masanori Nishikawa[d], Masahiro Nakayama[e], Keisei Kawa[b]

[a]*Department of Pediatric Surgery, Jichi Medical School, Minamikawachi-machi, Tochigi, 329-0498, Japan*
[b]*Department of Pediatrics, Osaka Medical Center and Research Institute for Maternal and Child Health, Izumi, Osaka, 565-0871, Japan*
[c]*Department of Pediatric Surgery, Osaka Medical Center and Research Institute for Maternal and Child Health, Izumi, Osaka, 565-0871, Japan*
[d]*Department of Radiology, Osaka Medical Center and Research Institute for Maternal and Child Health, Izumi, Osaka, 565-0871, Japan*
[e]*Department of Pathology, Osaka Medical Center and Research Institute for Maternal and Child Health, Izumi, Osaka, 565-0871, Japan*

Index words:
Neuroblastoma;
Mass screening;
Spontaneous regression;
Observation

Abstract

Background/Purpose: Neuroblastoma (NB) detected by mass screening (MS) usually shows favorable prognosis and sometimes regresses spontaneously. Therefore, the authors started an observation program for these patients to avoid overtreatment. In this study, the authors analyzed the profile of NB resected after observation to elucidate the nature of NB detected by MS.

Methods: Between 1994 and 2004, 22 NB patients matched the following criteria and entered the observation program after obtaining informed consent: stage I or II, less than 5 cm in diameter, and without involvement of large vessels or organs. If increase in size, elevation of tumor markers, or evidence of metastasis was observed, the tumor was immediately resected.

Results: Thirteen (59%) of 22 cases showed spontaneous regression. In the remaining 9 cases, tumors were resected because of parents' request, increase in size, and/or elevation of tumor markers. Four tumors had at least one unfavorable biologic feature, and 3 of them had more than 2. According to Shimada's system, 2 had unfavorable histology. One was diploid tumor, 3 had 1p deletion, and Trk-A expression was low in 4 tumors. All patients survived without evidence of recurrence.

Conclusions: The observation program has shown that at least one third of the NB detected by MS regressed spontaneously. On the other hand, MS may detect some cases with unfavorable tumor in early stage, which benefit from screening.

Presented at the 51st Annual Congress of the British Association of Paediatric Surgeons, Oxford, England, July 27-30, 2004.

* Corresponding author. Department of Pediatric Surgery, Jichi Medical School, Minamikawachi-machi, Tochigi-ken, 329-0498, Japan. Tel.: +81 285 58 7371; fax: +81 285 44 3234.
E-mail address: oue@jichi.ac.jp (T. Oue).

0022-3468/05/4002-0012$30.00/0
doi:10.1016/j.jpedsurg.2004.10.062

The prognosis of neuroblastoma (NB) in younger than 1 year is much better than that older than 1 year. In 1985, Japanese nationwide mass screening (MS) using urinary vanillyl mandelic acid (VMA) and homovanillic acid (HVA) for 6-month-old infants was started to improve the prognosis of this tumor [1]. Since then, more than 2000 patients with NBs were discovered and treated. Their prognosis was extremely good: more than 97% of them are alive [2]. Moreover, the majority of the NBs in MS group were biologically favorable even in advanced stages [3]. Recent reports have also shown that NB detected by MS sometimes regresses spontaneously [4,5]. Although the incidence of NB has remarkably increased after introduction of MS, several reports suggest that the number of advanced NB patients older than 1 year has not decreased substantially [3]. These findings indicate that MS has detected tumors that otherwise may have regressed spontaneously without recognition [4,5]. Therefore, we started an observation program in the limited cases to avoid overtreatment and to estimate how frequently regression occurs (Wait and

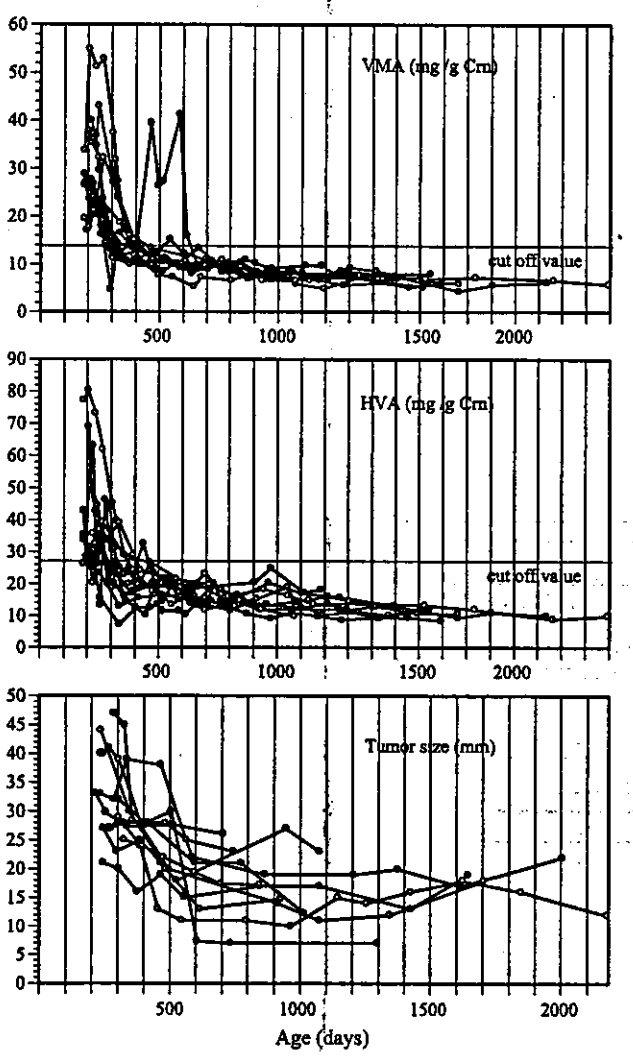

Fig. 1 Changes in levels of VMA and HVA, and tumor size in regressed cases.

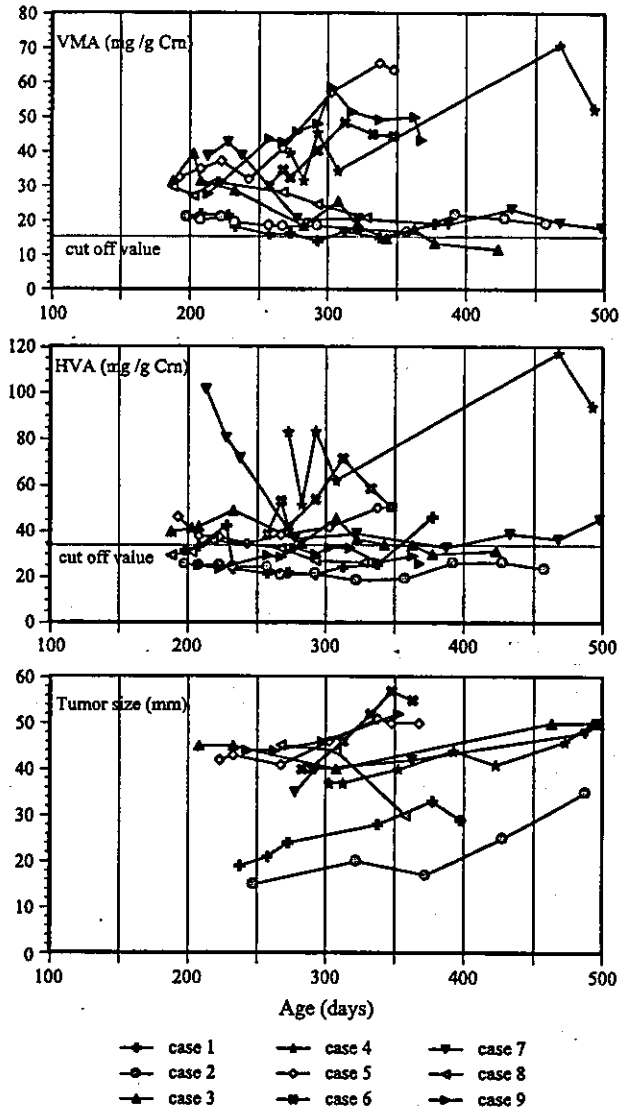

Fig. 2 Changes in levels of VMA and HVA, and tumor size in regressed cases. The cutoff values of urinary VMA/HVA levels were 12.6 and 27.0 mg/g Crn, respectively.

See pilot study) in June 1994 [6]. Our preliminary results have shown that at least 60% of NB cases who entered our observation program regressed spontaneously [6]. In this study, we analyzed the profile of NB resected after observation to elucidate the nature of NB detected by MS.

1. Patients and methods

The details of our observation program have been described previously [6]. The entry criteria were as follows: (1) stage I and II [7], (2) less than 5 cm in diameter, (3) no involvement of large vessels or organs and surgical resection is not difficult, and (4) parents' informed consent. The patients were strictly followed up without receiving any treatment. If increase in size, elevation of tumor markers, or evidence of metastasis was observed, the tumor was

Table 1 Neuroblastoma resected after observation

Case	Stage	Origin	Initial			Preoperative			Reason of interruption	Obs days	Age at ope (mo)
			VMA	HVA	Size	VMA	HVA	Size			
1	IVs	Lt retro	21.1	31.6	19	19.0	46.3	33	Size ↑, marker ↑	199	13
2	I	Lt retro	21.0	25.5	15	19.1	23.7	25	Size ↑, parents' request ↑	291	16
3	I	Lt adrenal	31.5	39.9	40	11.7	31.5	50	Size ↑	309	16
4	I→III	Lt adrenal	39.5	83.3	37	52.4	94.5	50	Size ↑, LN meta ↑	226	16
5	I→II	Rt adrenal	32.5	46.3	42	63.7	50.9	50	Size ↑, marker ↑	174	11
6	I	Lt adrenal	30.0	38.7	40	44.4	50.6	57	Size ↑, marker ↑	96	11
7	II	Rt retro	38.6	101.5	35	18.0	45.4	50	Size ↑	300	16
8	I	Rt adrenal	29.7	29.5	45	20.9	26.7	40	Parents' request	172	11
9	I→III	Rt retro	27.6	25.0	44	43.3	26.0	52	Size ↑	159	12

Size indicates longer diameter (mm); stage, Evans' staging system [7]; Lt, left; Rt, right; retro, retroperitoneum; LN meta, lymph node metastasis; obs, observation; ope, operation.

resected immediately. Biological features of the tumor were identified: Shimada's histological features [7], amplification of N-*myc* (Southern blotting, SRL Inc, Tokyo, Japan), 1p deletion (FISH, Otsuka Assay Laboratory, Tokyo, Japan), and expression of Trk-A (immunohistochemistry) [8]. Between June 1994 and March 2004, 43 patients with NB detected by MS were admitted to our hospital, and 22 (51 %) of them matched the criteria and were enrolled in the observation program. They included 11 boys and 11 girls. Age at diagnosis ranged from 7 to 11 months. Origins of the tumors were adrenal grand in 15 and retroperitoneal paraganglion in 7. Seventeen cases were in stage I, and 3 in stage II. Two patients in stage IV were also enrolled in the study, because the parents refused any treatment.

2. Results

Thirteen (59%) of 22 cases showed spontaneous regression and continued the observation program. The observation periods ranged from 15 to 116 months until May 2004. Urinary levels of VMA and HVA decreased and normalized within 18 months in all cases except one (Fig. 1). The tumor size (maximum diameter) was decreased to 0.7 to 2 cm within 3 years in all the cases; however, no tumor has disappeared (Fig. 1). In the remaining 9 (41%) cases, tumor resection was performed in 96 to 309 days after initial screening. In 2 cases, parents decided to stop the observation; therefore, the tumors were resected after 291- and 172-day observation. The remaining 7 tumors were resected because of increase in size and/or elevation of tumor markers (Fig. 2). In 2 cases (cases 4 and 5), lymph node metastases were observed at operation, resulting in the upgrading of the tumor stage from I to II and I to III, respectively. In case 9, tumor growth resulted in the upgrading of stage from I to III. The profile of the resected cases is listed in Tables 1 and 2. Four tumors (cases 2, 3, 7, and 8) showed differentiation to ganglioneuroblastoma. Biological features of the 9 resected tumors were listed in Table 2. According to Shimada's system, 7 were favorable, and 2 were unfavorable. DNA content was aneuploid in 7 tumors and diploid in one. Three of them had 1p deletion. Trk-A expression was low in 4 cases. Two cases (cases 6 and 7) showed biological heterogeneity in the tumor. No tumor showed N-*myc* amplification. Four (44%) tumors had at least one unfavorable biologic feature, and 3 of 4 tumors had more than 2 features. All tumors were resected completely without major surgical complication. Two of

Table 2 Neuroblastoma resected after observation

Case	His	Shimada's classification	N-*myc* (copy)	DNA ploidy	1p deletion	Trk-A expression	Operative procedure	Post operative chemotherapy
1	NB	Unfavorable	1	A	–	Low	Open	+
2	GNB	Favorable	1	A	–	High	Open	–
3	GNB	Favorable	1	ND	–	High	Laparoscopic	–
4	NB	Favorable	1	A	–	High	Open	+
5	NB	Favorable	1	A	+	Low	Open	–
6*	NB	Favorable	1	A/D	+	High/low	Open	–
7*	GNB	Unfavorable	1	A/A	+/–	Low/low	Open	+
8	GNB	Favorable	1	A	ND	ND	Laparoscopic	–
9	NB	Favorable	1	A	–	ND	Open	+

His indicates histology; GNB, ganglioneuroblastoma; ND, not detected; A, aneuploid; D, diploid.
* Showed intratumoral heterogeneity.

them were resected laparoscopically. Postoperative chemotherapy was performed in 4 cases who had stage III tumor and/or unfavorable prognostic factors. All patients survived without evidence of recurrence.

3. Discussion

In the presented series, among 43 NBs detected by MS, 22 have entered the observation program, and 13 tumors regressed spontaneously. Therefore, tumors are expected to regress at least in 59% of the patients who fulfilled our observation program or in 29% of all the patients detected by MS. Moreover, 5 of the 9 resected tumors had favorable biologic feature, which indicate that they have possibility of spontaneous regression if observation was continued. Therefore, the incidence of spontaneous regression should be higher. Similar observation trials were made at other institutes; Nishihira et al [5] reported that 17 (65%) tumors of 26 patients who were enrolled in their observation program regressed. Yamamoto et al [4] reported that 92% of the observed tumors or 44% of all the tumors identified by MS have spontaneously regressed. These results suggested that at least one third of the NB detected by MS might regress spontaneously. To avoid the overtreatment, several trials have been introduced including laparoscopic surgery [9] and reduction of chemotherapy [5]. We consider that observation program is most effective to avoid the unnecessary treatment.

Most of screened NBs were biologically favorable. However, there was a small group with biologically unfavorable factors, such as diploid DNA content, chromosomal pattern with 1p deletion, lower Trk-A expression, and N-*myc* amplification. Suita et al reported that 5 of 285 NBs detected by MS had amplified N-*myc* oncogene, 4 of 74 showed unfavorable Shimada's histological findings, and 3 of 33 had an unfavorable DNA ploidy pattern [3]. Therefore, MS may detect 2 biologically different groups, described as favorable and unfavorable. The unfavorable tumors may progress and/or disseminate in the future. Mass screening enables the cases with unfavorable tumor to undergo early treatment; therefore, these cases may benefit from MS. The favorable and unfavorable group can be identified only after analysis for the surgically removed tumor specimens. Therefore, identification of new prognostic factors that could distinguish the regressing tumor without surgery is required. Our examinations of the resected tumors after observation revealed high incidence of unfavorable biologic factors and upgrading of the tumor stage. Four (44%) of 9 resected tumors had at least one unfavorable biological feature. This percentage is much higher than reported percentage (0% to 20%) among all of the NBs detected by MS [3,10]. These findings suggest that unfavorable tumor may grow in size; therefore, they can be distinguished from the regressing tumors and be resected if they enter the observation program.

To clarify the benefits of MS in public health, we should prove whether MS decreases the number of advanced tumors and improves the survival. Several reports suggested that MS did not improve the overall mortality rate of NB [3]. Moreover, the results of the present study have proven that MS detects a considerable number of regressing tumors. Treatment of the regressing tumors may extremely harm the significance and cost benefit of MS, because the patients with regressing tumors had not received any treatment if MS would not have detected them. Based on the information obtained so far, the MS for NB at 6 months of age probably should not contribute to the public health. Therefore, Japanese Ministry of Health and Welfare has decided to discontinue the MS for NB at 6 months of age in April 2004. At the same time, our observation program at 6 months of age was also closed.

The optimal time for MS should be the point at which NB regressing spontaneously can no longer be detected, but more aggressive tumors can be found. Our observation program may determine the optimal timing of screening. Urinary VMA and HVA levels were normalized within 18 months in most of the regressed cases (Fig. 1). On the other hand, in the patients whose tumor increased in size, VMA and HVA levels were over the cutoff value at the time of operation. These findings suggest that screening in age around 18 months may be more effective; most of the favorable tumor has regressed, and unfavorable tumor should be detected. Now we are planning to start the new MS program for 18-month-old infants in Osaka prefecture, expecting to clarify whether MS in older age has benefit or not.

Acknowledgment

The authors thank Dr Tanaka of National Kure Hospital for detection of Trk-A expression.

References

[1] Sawada T, Matsumura T, Kawakatsu H, et al. Long-term effects of mass screening for neuroblastoma in infancy. Am J Pediatr Hematol/Oncol 1991;13:3-7.

[2] Matsumura T, Shikata T, Sawada T. Treatment modality for neuroblastoma infants in Japan: retrospective analysis and future directions. Proceedings of the 31st American Society of Clinical Oncology. J Clin Oncol 1995;14:456.

[3] Suita S, Zaizen Y, Sera Y, et al. Mass screening for neuroblastoma: quo vadis? A 9-year experience from the Pediatric Oncology Study Group of the Kyushu area in Japan. J Pediatr Surg 1996;31:555-8.

[4] Yamamoto K, Hanada R, Kikuchi A, et al. Spontaneous regression of localized neuroblastoma detected by mass screening. J Clin Oncol 1998;16:1265-9.

[5] Nishihira H, Toyoda Y, Tanaka Y, et al. Natural course of neuroblastoma detected by mass screening: 5-year prospective study at a single institution. J Clin Oncol 2000;18:3012-7.

[6] Yoneda A, Oue T, Imura K, et al. Observation of untreated patients with neuroblastoma detected by mass screening: a "wait and see" pilot study. Med Pediatr Oncol 2001;36:160-2.

[7] Evans AE, D'Angio GJ, Randolph J. A proposed staging for children with neuroblastoma. Children's Cancer Study Group A. Cancer 1995;27:374-8.
[8] Shimada H, Chatten J, Newton HW, et al. Histologic prognostic factors in neuroblastic tumors; Definition of subtypes of ganglioneuroblastoma and an age-linked classification of neuroblastoma. J Natl Cancer Inst 1984;73:405-16.
[9] Iwanaka T, Arai M, Ito M, et al. Surgical treatment for abdominal neuroblastoma in the laparoscopic era. Surg Endosc 2001;15:751-4.
[10] Tanaka T, Sugimoto T, Sawada T. Prognostic discrimination among neuroblastomas according to Ha-ras/Trk A gene expression: a comparison of the profiles of neuroblastomas detected clinically and those detected through mass screening. Cancer 1998;83:1626-33.

Int. J. Cancer: **112**, 365–375 (2004)

Publication of the International Union Against Cancer

LOW EXPRESSION OF HUMAN TUBULIN TYROSINE LIGASE AND SUPPRESSED TUBULIN TYROSINATION/DETYROSINATION CYCLE ARE ASSOCIATED WITH IMPAIRED NEURONAL DIFFERENTIATION IN NEUROBLASTOMAS WITH POOR PROGNOSIS

Chiaki KATO[1,2], Kou MIYAZAKI[1], Atsuko NAKAGAWA[3], Miki OHIRA[1], Yohko NAKAMURA[1], Toshinori OZAKI[1], Toshio IMAI[2] and Akira NAKAGAWARA[1]*

[1]*Division of Biochemistry, Chiba Cancer Center Research Institute, Chiba, Japan*
[2]*Department of Physiologic Chemistry Faculty of Science, Toho University, Chiba, Japan*
[3]*Second Department of Pathology, Aichi Medical University, Nagakute, Japan*

Neuroblastoma (NBL), one of the most common childhood solid tumors, has a distinct nature in different prognostic subgroups. However, the precise mechanism underlying this phenomenon remains largely unknown. To understand the molecular and genetic bases of neuroblastoma, we have generated its cDNA libraries and identified a human ortholog of *tubulin tyrosine ligase* gene (*hTTL/Nbla0660*) as a differentially expressed gene at high levels in a favorable subset of the tumor. Tubulin is subjected to several types of evolutionarily conserved posttranslational modification, including tyrosination and detyrosination. Tubulin tyrosine ligase catalyzes ligation of the tyrosine residue to the COOH terminus of the detyrosinated form of α-tubulin. The measurement of *hTTL* mRNA expression in 74 primary neuroblastomas by quantitative real-time reverse transcription-PCR revealed that its high expression was significantly associated with favorable stages (1, 2 and 4s; $p = 0.0069$), high *TrkA* expression ($p = 0.002$), a single copy of *MYCN* ($p < 0.00005$), tumors found by mass screening ($p = 0.0042$), nonadrenal origin ($p = 0.0042$) and good prognosis ($p = 0.023$). The log-rank test showed that high expression of *hTTL* was an indicator of favorable prognosis ($p = 0.026$). Immunohistochemical analysis using specific antibodies generated by us demonstrated that tyrosinated tubulin (Tyr-tubulin), detyrosinated tubulin (Glu-tubulin) and hTTL as well as Δ2-tubulin were positive in favorable tumors, whereas only Δ2-tubulin was positive in the tumors with *MYCN* amplification. In an RTBM1 neuroblastoma cell line, hTTL was increased after treating the cells with bone morphogenetic protein 2 (BMP2) or all-trans retinoic acid (RA), which induced neuronal differentiation. These results suggest that the deregulated tubulin tyrosination/detyrosination cycle caused by decreased expression of hTTL is associated with inhibition of neuronal differentiation and enhancement of cell growth in the primary neuroblastomas with poor outcome.

Key words: *tubulin tyrosine ligase; tubulin tyrosination; neuroblastoma; neuronal differentiation; prognostic factor*

Tubulin is one of the most important molecular components that regulate cytoskeletal structure relating to cell motility, cell division, differentiation, invasion and metastasis in cancer. However, functional modification of tubulin protein has still been elusive. Tubulin is subjected to several types of evolutionarily conserved posttranslational modification that includes tyrosination/detyrosination, acetylation, phosophorylation, palmitoylation, polyglutamylation and polyglycylation.[1–4] The discovery of tyrosination cycle stems from the serial observations that the addition of radiolabeled tyrosine to a rat brain cytosolic extract leads to tyrosination of the COOH terminus of a single endogenous protein, α-tubulin, by a translation-independent mechanism.[5–7] Posttranslational incorporation of tyrosine into the tubulin has also been shown to occur *in vivo*.[8–10] The cycle of tyrosination/detyrosination is evolutionarily conserved[11–13] and is regulated by both tubulin tyrosine ligase (TTL) and carboxypeptidase, the gene of which has not yet been identified (Fig. 1). Microtubule dynamics is also an important factor. TTL protein was first purified by immunoaffinity chromatography from the lysates of bovine and porcine brains and was extensively characterized by protein sequencing.[14] Recently, rat *TTL* cDNA has also been isolated.[15] Interestingly, in 1991, Paturle-Lafanechere *et al.*[16] identified a nontyrosinatable variant of tubulin that lacked 2 amino acid residues, glutamic acid and tyrosine, at the COOH terminus (Δ2-tubulin). Δ2-tubulin was found to accumulate in mature neurons and in stable microtubule assemblies in cells.[17,18] In some tumors, it also accumulated in the cellular cytoplasm in association with decreased levels of TTL, suggesting that the amount of Δ2-tubulin and TTL expression level in tumor cells are important to define the malignant grade of cancer.[19] However, pathophysiologic significance of the tyrosination/detyrosination cycle in normal and cancer cells still remains unclear.

Neuroblastoma (NBL) is one of the most common childhood solid tumors and has distinct biologic characteristics in different prognostic subgroups. For example, NBL in patients under 1 year of age usually regresses spontaneously, whereas that in patients over 1 year of age often grows aggressively and eventually kills the patient. To understand the molecular mechanism of distinct biology and tumorigenesis of NBL, we have previously performed a comprehensive approach to unveil the gene expression profiles among the NBL subsets.[20,21] We constructed the subset-specific oligo-capping cDNA libraries from the primary NBL tissues with favorable (stage 1, high expression of *TrkA* and a single copy of *MYCN*) and unfavorable (stage 3 or 4, decreased expression of *TrkA* and *MYCN* amplification) characteristics and randomly cloned 4,654 cDNAs. After adding the cDNAs obtained from the stage 4s NBL cDNA library to our NBL gene collection, we made an in-house cDNA microarray carrying 5,340 genes proper to NBL. The comprehensive analysis of 136 NBLs using the microar-

Abbreviations: BMP2, bone morphogenetic protein 2; DMEM, Dulbecco's modified Eagle's medium; ECL, enhanced chemiluminescence; FBS, fetal bovine serum; hTTL, human tubulin tyrosine ligase; NBL, neuroblastoma; RA, retinoic acid; TCP, tubulin carboxypeptidase; TTL, tubulin tyrosine ligase.

Grant sponsor: Grant-in-Aid for Scientific Research and for Scientific Research on Priority Areas, Medical Genome Science from the Ministry of Education, Science, Sports and Culture, Japan; Grant sponsor: Hisamitsu Pharmaceutical Co. Inc.

*Correspondence to: Division of Biochemistry, Chiba Cancer Center Research Institute, 666-2 Nitona, Chuoh-ku, Chiba 260-8717, Japan. Fax: +81-43-265-4459. E-mail: akiranak@chiba-ccri.chuo.chiba.jp

Received 27 January 2004; Accepted 15 April 2004

DOI 10.1002/ijc.20431
Published online 23 June 2004 in Wiley InterScience (www.interscience.wiley.com).

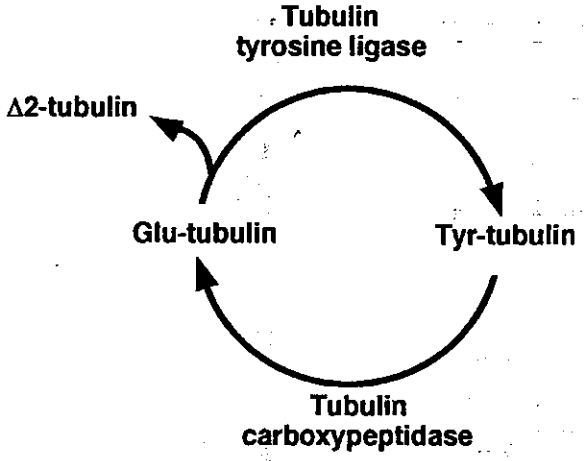

FIGURE 1 – The tyrosination/detyrosination cycle catalyzed by tubulin tyrosine ligase and tubulin carboxypeptidase.

ray showed that many genes that are related to the cytoskeletal components, including α-tubulin, had prognostic significance (data not shown).

In the present study, we have cloned for the first time the human ortholog of TTL (*hTTL*) from both the NBL and a fetal brain cDNA libraries. The analysis using 74 primary NBLs shows that expression of *hTTL* mRNA is significantly lower in unfavorable NBLs than in favorable tumors. The examination using specific antibodies raised against hTTL, Tyr-tubulin, Glu-tubulin and Δ2-tubulin demonstrates that hTTL is increased during induction of neuronal differentiation of cultured NBL cells treated with BMP2 or RA. The immunohistochemical study shows that hTTL, Tyr-tubulin, Glu-tubulin and Δ2-tubulin are positive in favorable NBLs, whereas only Δ2-tubulin is positive in aggressive NBLs with *MYCN* amplification. These suggested that the tyrosination/detyrosination cycle of α-tubulin is active in NBLs with high potential to differentiate or undergo apoptosis, while it is disregulated by downregulation of hTTL in *MYCN*-amplified NBLs, resulting in accumulation of Δ2-tubulin.

MATERIAL AND METHODS

Tumor specimen

Fresh frozen tumor tissues obtained by surgery or biopsy were sent to the Division of Biochemistry, Chiba Cancer Center Research Institute, from various hospitals in Japan with informed consent. Ninety tumors examined in this study were staged according to the International Neuroblastoma Staging System (INSS).[22] The number of tumors subjected to quantitative real-time RT-PCR were 24 in stage 1, 11 in stage 2, 5 in stage 4s, 10 in stage 3 and 24 in stage 4. The patients were treated according to the protocols previously described.[23] Biologic information on each tumor, including *MYCN* gene copy number, *TrkA* gene expression and DNA ploidy, was analyzed in our laboratory as described previously.[24]

Cell culture and transfection

COS7 and HEK293T cells were maintained in Dulbecco's modified Eagle's medium (DMEM) supplemented with 10% heat-inactivated fetal bovine serum (FBS; Life Technologies, Gaithersburg, MD) and penicillin (100 IU/ml)/streptomycin (100 μg/ml). Human neuroblastoma RTBM1 cells were grown in RPMI-1640 medium containing 10% heat-inactivated FBS and antibiotic mixture. Cultures were maintained at 37°C in a water-saturated atmosphere of 5% CO_2 in air. Transient transfection was performed by LipofectAMINE 2000 transfection reagent (Invitrogen, Carlsbad, CA) according to the manufacturer's instructions. In brief, cells were seeded in tissue culture plates to achieve 50% confluence. Twenty-four hours later, cells were transfected by using a mixture of the expression plasmids and LipofectAMINE 2000 transfection reagent in DMEM without serum. Forty-eight hours after transfection, cells were collected and analyzed by Western blotting. For neurite extension assays, RTBM1 cells were treated either with recombinant human BMP2 (Yamanouchi Pharmaceutical, Tokyo, Japan) or with RA at a final concentration of 1 nM or 5 μM, respectively.

RNA isolation and semiquantitative RT-PCR

Total RNA was prepared from neuroblastoma tissues according to the AGPC method.[25] Five micrograms of total RNA were subjected to the synthesis of the first-strand cDNA with pd$(N)_6$ random hexamer (Takara Shuzo, Otsu, Japan) and a Superscript II reverse transcriptase (Invitrogen) at 42°C for 90 min. The resultant cDNA was diluted to be a 1:20 solution and was amplified in a final volume of 10 μl of reaction mixture containing 100 μM of each deoxynucleoside triphosphate, 1 × PCR buffer, 1 μM of each primer and 0.2 U of rTaq DNA polymerase (Takara Bio, Ohtsu, Japan). The following primers were used: *hTTL*, 5′-CAGCTCTTCGGCTTTGACTT-3′ (sense) and 5′-GCTGTGGGCTGGATAAAGAG-3′ (antisense); human *GAPDH*, 5′-ACCTGACCTGCCGTCTAGAA-3′ (sense) and 5′-TCC ACCACCCTGTTGCTGTA-3′ (antisense). PCR templates were standardized by its *GAPDH* expression before performing semiquantitative PCR experiment. The PCR-amplified products were separated by electrophoresis on a 1.5% agarose gel and visualized by ethidium bromide poststaining.

Quantitative real-time RT-PCR

cDNA was prepared by the same method as in the semiquantitative RT-PCR and 2 μl of the 40-fold dilution was used for each PCR reaction. Primers and TaqMan probes for *hTTL* were designed using the primer design software Primer Express (Perkin-Elmer Applied Biosystems, Foster City, CA). The primer sequences for *hTTL* are 5′-AAGGAACTGCCTCCTGAGC-3′ and 5′-TCAATGAGCCAC ACCTTCA-3′. The probe sequence for *TTL* is 5′-FAM-ATTAGC ACCAAGCACCTCCCTTACCAGAGC-TAMRA-3′. PCR was carried out with the ABI Prism 7700 Sequence Detection System (Perkin-Elmer Applied Biosystems). Two μl of cDNA was amplified in a final volume of 25 μl containing 1 × TaqMan mixture, 300 nM each primer and 200 nM TaqMan probe. The thermal cycling condition was as follows: 50 cycles of a 2-step PCR (95°C for 15 sec, 60°C for 1 min) after the initial activation of UNG followed by denaturation (50°C for 2 min, 95°C for 10 min). TaqMan *GAPDH* control reagent kit (Roche Molecular Biochemicals, Basel, Switzerland) was used for the amplification of *GAPDH* according to the manufacturer's instructions; all data were normalized using *GAPDH* expression. The experiments were performed in triplicate for each data point.

Generation of polyclonal anti-hTTL antibodies

The polyclonal anti-hTTL antibody was raised in rabbits against Cys-coupled synthetic peptides derived from hTTL (222-RTASEPY-HVDNFQDKTCHLTNH-243 and 244-CIQKEYSKNYGKYEE-GNE-261). The polyclonal anti-Tyr-tubulin, anti-Glu-tubulin and anti-Δ2-tubulin antibodies were raised in rabbits immunized with Cys-coupled synthetic peptides corresponding to their COOH termini (CEEEGEEY, CGEEEGEE and CEGEEEGE, respectively). Antibodies were purified by using peptide-coupled affinity columns and tested for their ability to identify the corresponding proteins by Western blots. The synthetic peptides and antibodies were generated by Protein Express (Chiba, Japan).

Construction of FLAG-tagged hTTL expression plasmid

The FLAG-tagged hTTL expression plasmid was generated by PCR amplification using the cDNA library derived from human fetal brain (Stratagene, La Jolla, CA) and an *hTTL* cDNA that lacked the 5′-portion encoding the NH_2 terminal region of hTTL as templates. The forward and reverse primers used were 5′-TAAATAGTCGACGATATCATGGACTACAAGGACGAC

GACGACAAGTACACCTTCGTGGTACGCGATGAGAACAGC AGCGTCTACGCCGAGGTCTCCCGGCTGCTCCTCGCCA-3′ (sequence encoding FLAG epitope tag is in boldface, and *Eco*RV recognition site is underlined) and 5′-TACATGTCGACGCGG CCGCTCACAGCTTGAT GAA-3′ (*Not*I restriction site is underlined). The resulting PCR product was gel-purified, digested with *Eco*RV and *Not*I, inserted into identical restriction sites of a mammalian expression plasmid pIRESpuro2 (Clontech Laboratories, Palo Alto, CA) and its nucleotide sequence was verified by automated dideoxy terminator cycle sequencing.

Western blot analysis

Cells were washed in ice-cold phosphate-buffered saline (PBS), collected by centrifugation and lysed in 1 × sample buffer. Equal amounts of whole-cell lysates were fractionated by SDS-polyacrylamide gel electrophoresis (SDS-PAGE), and electrophoretically transferred onto a polyvinylidene difluoride (PVDF) membrane filter (Immobilon-P; Millipore, Billerica, MA). The filter was then blocked with Tris-buffered saline (TBS) containing 5% nonfat dry milk at room temperature for 1 hr and subsequently incubated for 1 hr with the antibodies against hTTL, Tyr-tubulin, Glu-tubulin, Δ2-tubulin, α-tubulin (5H1; PharMingen, San Diego, CA) and actin (20-33; Sigma Chemical, St. Louis, MO). The filter was further incubated with horseradish peroxidase-conjugated mouse or rabbit IgG secondary antibody (Cell Signaling Technologies, Beverly, MA). Immunoreactivity was detected using the enhanced chemiluminescence system (ECL; Amersham Pharmacia Biotechnology, Uppsala, Sweden) according to the manufacturer's instructions. The films were exposed at multiple time points to ensure that the images were not saturated.

Immunohistochemistry

Immunohistochemical stainings with antibodies against hTTL (1:100), Tyr-tubulin (1:100), Glu-tubulin (1:100) and Δ2-tubulin (1:100) were performed on 10 human neuroblastoma tumors selected from the surgical pathology file at the Department of Pathology, Aichi Medical University, based on the results of histopathology evaluation[26] and *MYCN* status. Also performed were immunostainings with antibodies against TrkA (1:40, 763; Santa Cruz Biotechnology, Santa Cruz, CA), CD56 (1B6; Novocastra Laboratories, Peterborough, U.K.) and Ki-67 (1:200, MIB-1; Dako, Kyoto, Japan) on the same tumor tissues. All of those tumor samples were obtained prior to chemotherapy and irradiation therapy and included 6 favorable histology cases with nonamplified *MYCN* (FH&NA) and 4 unfavorable histology cases with amplified *MYCN* (UH&A). Among the neuroblastoma cases, tumors in the FH&NA subset were reported to be the most favorable biologically and clinically. In contrast, tumors in the UH&A subset are known to be the most aggressive with the poorest clinical outcome.[27] Four μm thick sections from the formalin-fixed and paraffin-embedded tissue samples were deparaffinized and microwaved for 3 × 5 min in Na-citrate buffer (pH 6.0) for antigen retrieval. The slides were first immersed in 0.3% hydrogen peroxide in methanol for 20 min and then in 10% normal goat serum for 30 min. The primary antibodies were then applied at 4°C overnight, followed by a standard staining procedure using the Vectastain ABC kit (Vector Laboratories, Burlingame, CA). Sections were counterstained with hematoxylin for light microscopic review and evaluation. hTTL, Tyr-tubulin, Glu-tubulin and Δ2-tubulin were always positively detected in the cytoplasm and neuritic processes of normal ganglion cells in the separate positive control sections as well as in the test sections as built-in control, whenever available. As for the negative controls of hTTL, Tyr-tubulin, Glu-tubulin, Δ2-tubulin and TrkA stainings, normal rabbit immunoglobulins (1:500 dilution, Vector Laboratories) were applied as the primary antibody. As for the negative controls of CD56 and Ki-67 stainings, we followed the staining procedure without the primary antibodies.

Statistical analysis

Student's *t*-tests were used to explore possible associations between *hTTL* expression and other factors, such as age. Since the values of the *hTTL* expression were skewed, a log transformation was used to achieve the normality when using *t*-test and Cox regression. The distinction between high and low levels of *hTTL* was based on the median value (low, *hTTL* < 95 e.u.; high, *hTTL* > 95 e.u.), regardless of tumor stage, *MYCN* copy number, or survival. Kaplan-Meier survival curves were calculated, and survival distributions were compared using the log-rank test. Cox regression models were used to explore associations between *hTTL* expression, age, *MYCN* amplification, mass screening, origin and survival. Statistical significance was declared if the *p*-value was < 0.05. Statistical analysis was performed using Stata 7.0. (Stata, College Station, TX).

RESULTS

Cloning and expression of hTTL *gene*

We have previously constructed oligo-capping cDNA libraries from 3 fresh human NBL tissues (stages 1 and 2; high *TrkA* expression and a single copy of *MYCN*), which were gradually undergoing spontaneous regression probably due to neuronal apoptosis.[20] Screening of 1,152 novel genes by reverse transcriptase (RT)-PCR revealed that 194 genes were expressed differentially between NBLs with favorable prognosis and those with unfavorable outcome. Among them, we detected a partial cDNA sequence (*Nbla00660*) corresponding to the human ortholog of *tubulin tyrosine ligase* (*hTTL*) gene. We then cloned the full-length *hTTL* cDNA using both conventional phage library screening and genome sequence-based RT-PCR procedure. The *hTTL* gene was mapped to chromosome 2q13 and consisted of 7 exons (Fig. 2*a*) with 377 predicted amino acids (Genbank/DDBJ accession number AB071393; Fig. 2*b*). Comparison of the deduced amino acid sequence of human *TTL* cDNA with those of mouse, rat, pig and cow showed identity by 94%, 94%, 93% and 94%, respectively. *hTTL* was ubiquitously expressed in various human tissues including heart, kidney, lung, colon, thymus, spleen, mammary gland, testis, prostate, brain, cerebellum, liver, fetal brain, fetal liver, adrenal gland and skeletal muscle (Fig. 2*c*). However, it was rather preferentially expressed in adult and fetal brains and lung.

Specific antibodies and catalytic activity of hTTL

To study the role of hTTL and the tyrosination/detyrosination cycle regulated by TTL in neuroblastoma, we generated specific antibodies against human Tyr-tubulin, Glu-tubulin and Δ2-tubulin based on the previous reports.[16,18,28] The PVDF membranes spotted with equal amount (1 μg) of synthetic peptides corresponding to COOH terminal 7 amino acid residues of Tyr-tubulin (CEEEGEEY), Glu-tubulin (CGEEEGEE) and Δ2-tubulin (CEGEEEGE) were immunoblotted with rabbit anti-Tyr-tubulin antibody (Fig. 3*a*, top), anti-Glu-tubulin antibody (Fig. 3*a*, middle) and anti-Δ2-tubulin antibody (Fig. 3*a*, bottom), respectively. There were no crossreactivities among them, suggesting that those 3 antibodies were highly specific to each form of tubulin. To confirm the catalytic activity of hTTL encoded by the gene we cloned, we transfected the HEK293T cells with various amount of *hTTL* expression construct. Increased levels of hTTL in those cells induced tyrosination of tubulin in dose-dependent manner, while the level of endogenous Glu-tubulin was decreased (Fig. 3*c*). These results showed that hTTL protein encoded by the gene we cloned has its catalytic activity.

Upregulation of hTTL expression during neuronal differentiation

BMP2 has been characterized as a neurotrophic factor.[29] Recently, Nakamura *et al.*[30] have reported that RTBM1, a human neuroblastoma cell line, is responsive to both BMP2 and RA by extending neurites. By using this system, we examined whether the expression levels of hTTL change during induction of neuronal differentiation. As shown in Figure 4, the treatment of RTBM1

a

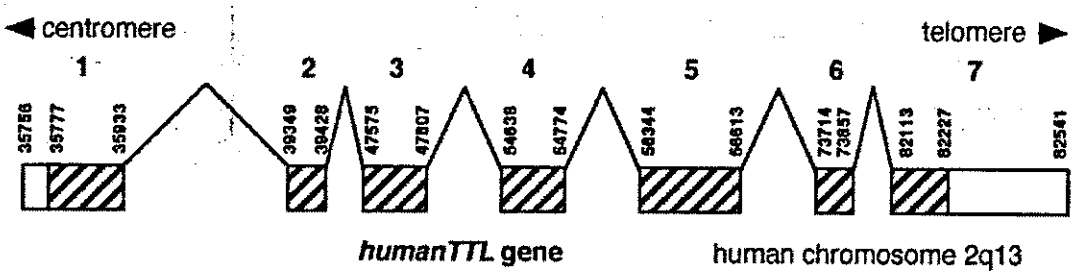

b

```
humanTTL  MYTFVVRDENSSVYAEVSRLLLATGHWKRLRRDNPRFNLMLGERNRLPFGRLGHEPGLVQLVNYYRGADKLCRKAS 76
mouseTTL  MYTFVVRDENSSVYAEVSRLLLATGYWKRLRRDNPRFNLMLGERNRLPFGRLGHEPGLAQLVNYYRGADKLCRKAS 76
ratTTL    MYTFVVRQENSSVYAEVSRLLLATGYWKRLRRDNPRFNLMLGGRNRLPFGRLGHEPGLAQLVNYYRGADKLCRKAS 76
pigTTL    MYTFVVRDENSSVYAEVSRLLLATGHWKRLRRDNPRFNLMLGERNRLPFGRLGHEPGLMQLVNYYRGADKLCRKAS 76
cowTTL    MYTFVVRDENSSVYAEVSRLLLATGHWKRLRRDNPRFNLMLGERNRLPFGRLGHEPGLMQLVNYYRGADKLCRKAS 76
          ******* ****************** ***************** ***************** ******************

humanTTL  LVKLIKTSPELAESCTWFPESYVIYPTNLKTPVAPAQNGIQPPISNSRTDEREFFLASYNRKKEDGEGNVWIAKSS 152
mouseTTL  LVKLVKTSPELSESCSWFPESYVIYPTNLKTPVAPAQNGIQLPVSNSRTDEREFFLASYNRKKEDGEGNVWIAKSS 152
ratTTL    LVKLVKTSPELSESCSWFPESYVIHPTNLKTPVAPAQNGIQLPVSNSRTDEREFFLASYNRKKEDGEGNVWIAKSS 152
pigTTL    LVKLIKTSPELAESCTWFPESYVIYPTNLKTPVAPAQNGIHPPIHSSRTDEREFFLTSYNKKKEDGEGNVWIAKSS 152
cowTTL    LVKLIKTSPELAESCTWFPESYVIYPTNLKTPVAPAQDGIHPPLHSSRTDEREFFLASYNRKKEEGEGNVWIAKSS 152
          **** ****** *** ******** ************ ** *  ********** *** *** ************

humanTTL  AGAKGEGILISSEASELLDFIDNQGQVHVIQKYLEHPLLLEPGHRKFDIRSWVLVDHQYNIYLYREGVLRTASEPY 228
mouseTTL  AGAKGEGILISSEASELLDFIDSQGQVHVIQKYLERPLLLEPGHRKFDIRSWVLVDHQYNIYLYREGVLRTASEPY 228
ratTTL    AGAKGEGILISSEASELLDFIDNQGQVHVIQKYLEHPLLLEPGHRKFDIRSWVLVDHQYNIYLYREGVLRTASEPY 228
pigTTL    AGAKGEGILISSEATELLDFIDNQGQVHVIQKYLERPLLLEPGHRKFDIRSWVLVDHQYNIYLYREGVLRTASEPY 228
cowTTL    AGAKGEGILISSDATELLDFIDNQGQVHVIQKYLERPLLLEPGHRKFDIRSWVLVDHQFNIYLYREGVLRTASEPY 228
          *********** * ******* ************ ********************** ******************

humanTTL  HVDNFQDKTCHLTNHCIQKEYSKNYGKYEEGNEMFFKEFNQYLTSALNITLESSILLQIKHIIRNCLLSVEPAIST 304
mouseTTL  HVDNFQDKTCHLTNHCIQKEYSKNYGKYEEGNEMFFEEFNQYLTSALNITLESSILLQIKHIIRSCLMSVEPAIST 304
ratTTL    HVDNFQDKTCHLTNHCIQKEYSKNYGKYEEGNEMFFEEFNQYLTSALNITLENSILLQIKHIIRSCLMSVEPAIST 304
pigTTL    HTDNFQDKTCHLTNHCIQKEYSKNYGKYEEGNEMFFEEFNQYLTSALNITLESSILLQIKHIIRSCLLSVEPAIST 304
cowTTL    HMDNFQDKTCHLTNHCIQKEYSKNYGKYEEGNEMFFEAFNRYLTSALNITLESSILLQIKHIIRSCLMSVEPAIST 304
          * ********************************** ** *********** *********** ** *********

humanTTL  KHLPYQSFQLFGFDFMVDEELKVWLIEVNGAPACAQKLYAELCQGIVDIAISSVFPPPDVEQPQTQP--AAFIKL  377
mouseTTL  KHLPYQSFQLLGFDFMVDEELKVWLIEVNGAPACAQKLYAELCQGIVDIAISSVFPPPDTEQVPQQP--AAFVKL  377
ratTTL    KHLPYQSFQLLGFDFMVDEELKVWLIEVNGAPACAQKLYAELCQGIVDIAISSVFPPPDTEQVPQQP--AAFMKL  377
pigTTL    RHLPYQSFQLFGFDFMVDEDLKVWLIEVNGAPACAQKLYAELCQGIVDIAIASVFPPPDAEQQQQQPPPAAFIKL  379
cowTTL    KHLPYQSFQLFGFDFMVDEELKVWLIEVNGAPACAQKLYAELCQGIVDIAIASVFPPPDAEQQPPQP--ATFIKL  377
          ********* ******** ********************************** ******* **   **  * * **
```

c

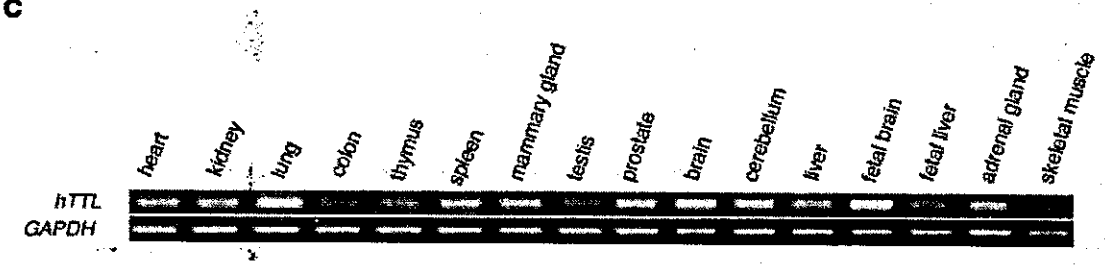

FIGURE 2